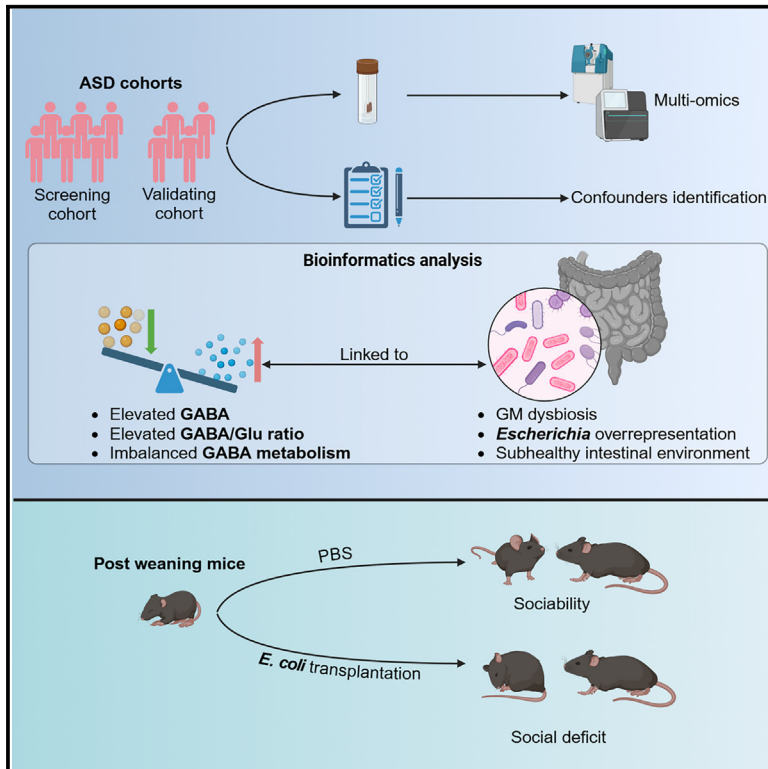**Article**

Gut microbial GABA imbalance emerges as a metabolic signature in mild autism spectrum disorder linked to overrepresented *Escherichia*

Graphical abstract

Authors

Dilong Wang, Youheng Jiang,
Jian Jiang, ..., Huiliang Li, Yulong He,
Ningning Li

Correspondence

xuesong.zhang@rutgers.edu (X.-S.Z.),
huiliang.li@ucl.ac.uk (H.L.),
heyulong@mail.sysu.edu.cn (Y.H.),
linn29@mail.sysu.edu.cn (N.L.)

In brief

Wang et al. find an elevated gut microbial GABA/glutamate ratio in children with ASD, establishing it as a marker associated with ASD diagnosis. They elucidate that abnormal GABA metabolism is linked to the overrepresentation of *Escherichia* in the gut. These findings provide insights into strategies aiming at restoring neurotransmitter homeostasis in ASD.

Highlights

- Features of imbalanced gut microbial GABA metabolism in preschool children with mild ASD

- Microbial GABA/glutamate ratio is potentially an independent marker for ASD diagnosis

- Overrepresentation of *Escherichia* is associated with abnormal GABA metabolism in ASD

- Simulated overgrowth of *E. coli* potentiates social deficits in mice

CellPress

Cell Reports Medicine

Article

Gut microbial GABA imbalance emerges as a metabolic signature in mild autism spectrum disorder linked to overrepresented *Escherichia*

Dilong Wang,[1,2,13] Youheng Jiang,[1,3,13] Jian Jiang,[1,4,13] Yihang Pan,[1,3,13] Yanming Yang,[1] Xiaoyi Fang,[5] Liyang Liang,[2] Hai Li,[6] Zepeng Dong,[1] Shilu Fan,[7] Daqing Ma,[8,9] Xue-Song Zhang,[10,*] Huiliang Li,[11,*] Yulong He,[1,3,*] and Ningning Li[1,12,14,*]

[1]Tomas Lindahl Nobel Laureate Laboratory, The Seventh Affiliated Hospital, Sun Yat-sen University, Shenzhen, Guangdong 518107, China
[2]Department of Pediatrics, Sun Yat-sen Memorial Hospital of Sun Yat-sen University, Guangzhou, Guangdong 510000, China
[3]Center for Digestive Disease, Guangdong Provincial Key Laboratory of Digestive Cancer Research, The Seventh Affiliated Hospital, Sun Yat-sen University, Shenzhen, Guangdong 518107, China
[4]Center for Clinical Molecular Medicine, National Clinical Research Center for Child Health and Disorders, Ministry of Education Key Laboratory of Child Development and Disorders, Children's Hospital of Chongqing Medical University, Chongqing 400014, China
[5]Department of Neonatology, The Seventh Affiliated Hospital of Sun Yat-sen University, Shenzhen, Guangdong 518107, China
[6]Neurorehabilitation Laboratory, Department of Rehabilitation Medicine, Shenzhen Hospital, Shenzhen, Guangdong 518107, China
[7]ARK Autism & Rehabilitation Institute, Taiyuan, Shanxi 030000, China
[8]Division of Anaesthetics, Pain Medicine and Intensive Care, Imperial College London, Chelsea and Westminster Hospital, London SW10 9NH, UK
[9]Perioperative and Systems Medicine Laboratory, Children's Hospital, Zhejiang University School of Medicine, Hangzhou 310003, China
[10]Center for Advanced Biotechnology and Medicine, Rutgers University, Piscataway, NJ 08854, USA
[11]Wolfson Institute for Biomedical Research, Division of Medicine, Faculty of Medical Sciences, University College London, London WC1E 6AE, UK
[12]China-UK Institute for Frontier Science, Shenzhen 518107, China
[13]These authors contributed equally
[14]Lead contact
*Correspondence: xuesong.zhang@rutgers.edu (X.-S.Z.), huiliang.li@ucl.ac.uk (H.L.), heyulong@mail.sysu.edu.cn (Y.H.), linn29@mail.sysu.edu.cn (N.L.)
https://doi.org/10.1016/j.xcrm.2024.101919

SUMMARY

Gut microbiota (GM) alterations have been implicated in autism spectrum disorder (ASD), yet the specific functional architecture remains elusive. Here, employing multi-omics approaches, we investigate stool samples from two distinct cohorts comprising 203 children with mild ASD or typical development. In our screening cohort, regression-based analysis for metabolomic profiling identifies an elevated γ-aminobutyric acid (GABA) to glutamate (Glu) ratio as a metabolic signature of ASD, independent of age and gender. In the validating cohort, we affirm the GABA/Glu ratio as an ASD diagnostic indicator after adjusting for geography, age, gender, and specific food-consuming frequency. Integrated analysis of metabolomics, 16S rRNA sequencing, and metagenomics reveals a correlation between overrepresented *Escherichia* and disrupted GABA metabolism. Furthermore, we observe social behavioral impairments in weaning mice transplanted with *E. coli*, suggesting a potential link to ASD symptomatology. Collectively, these findings provide insights into potential diagnostic and therapeutic strategies aimed at evaluating and restoring gut microbial neurotransmitter homeostasis.

INTRODUCTION

Autism spectrum disorder (ASD), characterized by impaired social interaction, repetitive behavior, and stereotyped interests, poses significant challenges to social adaptability in affected individuals.[1] With a global prevalence recently estimated at 1%–2%,[2] ASD imposes a substantial social burden. Early intervention is widely acknowledged as crucial for positive outcomes,[3] yet diagnosing ASD in young children remains challenging due

to the disorder's heterogeneous symptomatology and limited expressive capacities in verbal and nonverbal communication.[4] The need for effective laboratory-based indices to elucidate ASD etiology and track its development is pressing.

Recent research has drawn attention to the potential role of gut microbiota (GM) in ASD pathogenesis. From the discovery of ASD-featured GM dysbiosis[5,6] to the observed alleviation of autistic symptoms through healthy GM transplantation,[7,8] accumulating evidence underscores the significance of GM in ASD. A

Table 1. Clinical characteristics of subjects with ASD and TD

	Screening cohort			Validating cohort		
	ASD	TD	p value	ASD	TD	p value
Subjects (n)	56	67	–	40	40	–
Average age (years)	5.05 (1.43)	4.58 (1.01)	0.13[b]	5.08 (1.42)	4.25 (1.15)	0.360[b]
Male proportion (%)	91.1	56.7	<0.001[c]	82.5	42.5	<0.001[c]
Severity (CARS[a])	34.63 (2.72)	–	–	34.1 (10.17)	–	–
Constipation (%)	42.86	26.87	0.085[c]	37.5	30	0.637[c]
Delivery (caesarean %)	39.29	38.81	1.000	27.5	12.5	0.161[c]

Data are presented as "mean (SD)," unless otherwise stated.
[a]CARS, Childhood Autism Rating Scale.
[b]p value = Wilcoxon rank-sum test between groups.
[c]p value = Chi-Square test between groups.

comprehensive analysis of GM characteristics associated with ASD at various levels is essential for identifying novel diagnostic biomarkers and therapeutic targets.

Despite significant efforts to characterize an ASD-specific GM structure in recent years, findings from various studies have demonstrated inconsistency and, at times, contradiction. For instance, a systematic review outlined a concurrent decrease in the abundances of *Bifidobacterium*, *Blautia*, *Dialister*, *Prevotella*, *Veillonella*, and *Turicibacter* in patients with ASD,[9] while according to a recent large-scale study, most of these genera remained unchanged in abundances, and *Bifidobacterium* was even increased in ASD.[10] This variability may arise from diverse covariates across studies, such as age, gender, geography, diet, antibiotic or prebiotic administration, and stool consistency. Except for these well-known confounders, altered GM composition was found to be linked to autistic behavioral issues,[11] which may conversely contribute to idiosyncratic dietary preferences and impact GM.[12] These findings suggest that ASD subtypes, typically categorized by severity, and other relevant factors should be taken into account during participant recruitment and data analysis.

Microbial metabolites form a dynamic network that contributes to the homeostasis of both the GM community and the host.[13,14] A recent analysis, utilizing multiple omics databases, has uncovered similarities between gut microbial metabolism and human brain metabolism in individuals with ASD.[15] This finding underscores the importance of exploring potential GM-host interactions via dissecting microbial metabolic profiles in ASD. While much of the evidence regarding the significance of microbial metabolites in ASD has stemmed from animal studies, compounds such as short-chain fatty acids (SCFAs), neurotransmitters, and bile acids (BAs) have been shown to influence social behavior by affecting energy metabolism, immune responses, and neuroactivity.[14,16] For instance, exposure to propionic acid has been linked to the development of autistic-like behaviors in rats,[17] while our research, along with that of others, has demonstrated that indole-3-propionic acid supplementation can alleviate social deficits in mouse models.[18,19] However, the metabolic signature of GM in autistic children remains inadequately characterized. Previous attempts using metagenomics have identified metabolic abnormalities in autistic GM related to genetic pathways involved in neurotransmitter synthesis[10,20–22] and detoxification.[23] Nevertheless, the levels of the relevant metabolites were often unmen-

tioned or unvalidated biochemically in these studies. Establishing a core ASD-associated metabolic profile of GM necessitates a cross-examination of evidence through multi-omics analyses. Meanwhile, concomitant verification in animal experiments would further reveal the role of GM dysbiosis in autistic symptoms.

In this study, we conducted multi-omics analyses to thoroughly examine metabolic, functional, and taxonomic changes in the GM of individuals with mild ASD compared to those with typical development (TD). We analyzed stool samples from 203 participants across both a screening and a validating cohort. The regression-based metabolomics analysis, after adjusting for covariates, revealed a significant increase in the ratio of γ-aminobutyric acid (GABA) to glutamate (Glu) in individuals with ASD. These findings established the increment of the GABA/Glu ratio as a metabolic signature in the screening cohort and as an independent indicator for ASD diagnosis in the validating cohort. Through an integrated analysis of metabolomics, 16S rRNA sequencing, and metagenomics, we identified an overrepresentation of the *Escherichia* genus, which was linked to abnormal GABA metabolism in the GM of individuals with ASD. Notably, experimental transplantation of *E. coli* into weaning mice induced social deficits, a hallmark of ASD.

RESULTS

Participant recruitment, sampling, and confounder identification

We focused on mild cases of ASD, which represent the predominant demographic globally in this patient population.[24–26] Further, our study was methodically designed in two distinct phases to effectively screen and validate the core microbial signatures associated with ASD. Herein, in the screening phase, we recruited a cohort of 123 children (56 ASD and 67 TD) from a dedicated ASD institute and adjacent communities (Table 1, screening cohort). The recruitment strategy in this phase was tailored to ensure homogeneity in environmental factors and demographic distribution among participants. A Childhood Autism Rating Scale evaluation verified that all subjects with ASD were indeed mild cases. To broaden the geographical diversity of our study, we formed a validating cohort, comprising 40 subjects with mild ASD from multiple institutes, along with geography-matched subjects with TD (Table 1, validating cohort).

Table 2. Logistic regression analysis for identifying confounding factors

	Factors	B	Wald	*p* value	OR
Screening cohort	age	0.30	4.06	0.044	1.35
	gender	−2.05	15.02	0.000	0.13
	batch	−0.60	1.24	0.265	0.55
	constipation	−0.71	3.42	0.064	0.49
	delivery	−0.02	0.00	0.957	0.98
	stool consistency	−0.73	3.31	0.069	0.48
Validating cohort	city	−0.20	0.20	0.653	0.82
	gender	−1.59	9.79	0.002	0.21
	age	0.33	3.54	0.060	1.39
	delivery	−0.11	0.06	0.813	0.89
	stool consistency	−0.09	0.19	0.665	0.91
	constipation	−0.98	2.69	0.101	0.38
	whole grain	0.08	0.36	0.547	1.08
	fruits	−0.38	4.75	0.029	0.68
	vegetables	−0.48	7.88	0.005	0.62
	dark vegetables	−0.38	5.38	0.020	0.69
	dairy products	−0.23	2.20	0.138	0.80
	beans	−0.43	3.51	0.061	0.65
	fungi and algae	−0.59	4.56	0.033	0.55
	fish	−0.43	2.19	0.139	0.65
	animal liver	0.64	2.06	0.151	1.89
	sugar-sweetened beverage	0.16	0.55	0.458	1.17
	fried foods	0.25	0.85	0.358	1.28
	western fast food	0.48	2.50	0.114	1.61
	breakfast	−0.29	2.19	0.139	0.75
	snacks	−0.02	0.02	0.881	0.98

In both the screening and validating cohorts, most participants were preschoolers aged 3 to 5 years, with a comparable mean age between the ASD and TD groups. The ASD groups displayed significantly higher male proportions compared to the TD groups. Both cohorts demonstrated comparable rates of constipation and caesarean births between the two groups.

During sampling, stool consistency was strictly controlled via collecting corn-on-cob-like and sausage-like fecal samples (Table S1), which are classified as normal as per the Bristol Stool Chart. In the screening cohort, a procedure of repeated sampling was performed for subsequent multiple-omics measurements. The first sampling collected 123 stool samples (ASD = 56, TD = 67), while the second sampling yielded 102 samples (ASD = 50, TD = 52) since 21 participants were lost to follow-up. In the validating cohort, 80 stool samples (ASD = 40, TD = 40) were collected.

To identify potential covariates associated with ASD diagnosis in the screening cohort, we performed a single-factor logistic regression analysis considering age, gender, sampling batch, mode of delivery, constipation condition, and stool consistency as independent variables. We found that age and gender were significantly associated with ASD diagnosis (Table 2; Figure S1A).

Given the importance of dietary habits as a major confounder in microbiome studies of ASD,[9] we collected additional dietary information in the validating cohort using a detailed questionnaire on weekly food consumption.[27,28] Our subsequent single-factor logistic regression analysis included residential city, gender, age, mode of delivery, constipation condition, and specific food consumption frequency as independent variables, with ASD diagnosis as the dependent variable. Notably, we observed distinct patterns between the two groups regarding gender and the consumption of specific foods, including fruits, vegetables, dark vegetables, fungi, and algae, which were associated with ASD diagnosis (Table 2).

Imbalanced metabolism of microbial GABA as an age- and gender-independent signature of ASD

To investigate the metabolic characteristics of GM in ASD, we first determined a total of 32 well-documented metabolites (Table S2, first sampling), including 10 neurotransmitters, 7 SCFAs, and 15 BAs that are broadly applicable to ASD symptomatology based on literature or clinical inference.[29] For metabolomics analysis, we utilized the first sampling from our screening cohort (Figure 1A, first sampling). To minimize analytic bias caused by confounders in the cohort, we applied the inverse normal transformation (INT) method[30] to achieve normally distributed metabolite levels adjusted for age and gender. Subsequent analysis using partial least-squares discriminant analysis (PLS-DA) revealed a clear separation of the metabolite profiles between individuals with ASD and TD (Figure 1B). Employing a threshold of $p < 0.05$, false discovery rate (FDR) < 0.1, and variable importance in projection > 1, we identified 6 differential metabolites: GABA, norepinephrine, dihydroxyphenylalanine, histidine, acetic acid, and glycolithocholic acid (Figure 1C). Notably, the most significant change among these differential metabolites was an increased level of GABA in individuals with ASD (Figure 1D).

To delve deeper into the alterations in GABA metabolism, we analyzed the second sampling from our screening cohort, focusing specifically on metabolites involved in GABA metabolism (Figure 1A, second sampling). We selected 10 metabolites, involved in GABA synthesis and decomposition, and applied the INT method to normalize the levels of these metabolites, adjusting for age and gender (Table S2, second sampling). PLS-DA plots demonstrated a clear separation of the metabolite profiles between the two groups (Figure 1E). Importantly, in keeping with the results from the first sampling, subjects with ASD exhibited a significant augment of GABA, along with notable declines in Glu, glutamine (Gln), and fumarate, compared to TD controls (Figure 1F). These results suggested a complex, ASD-specific fluctuation in GABA metabolism.

To comprehensively encapsulate this metabolic trait, we calculated the ratios of GABA to Glu and Glu to Gln using data from our first sampling. These ratios serve to recapitulate the dynamics of GABA metabolism (Table S2, ratios). Additionally, to capture key features of microbial metabolism in ASD from a broader range,
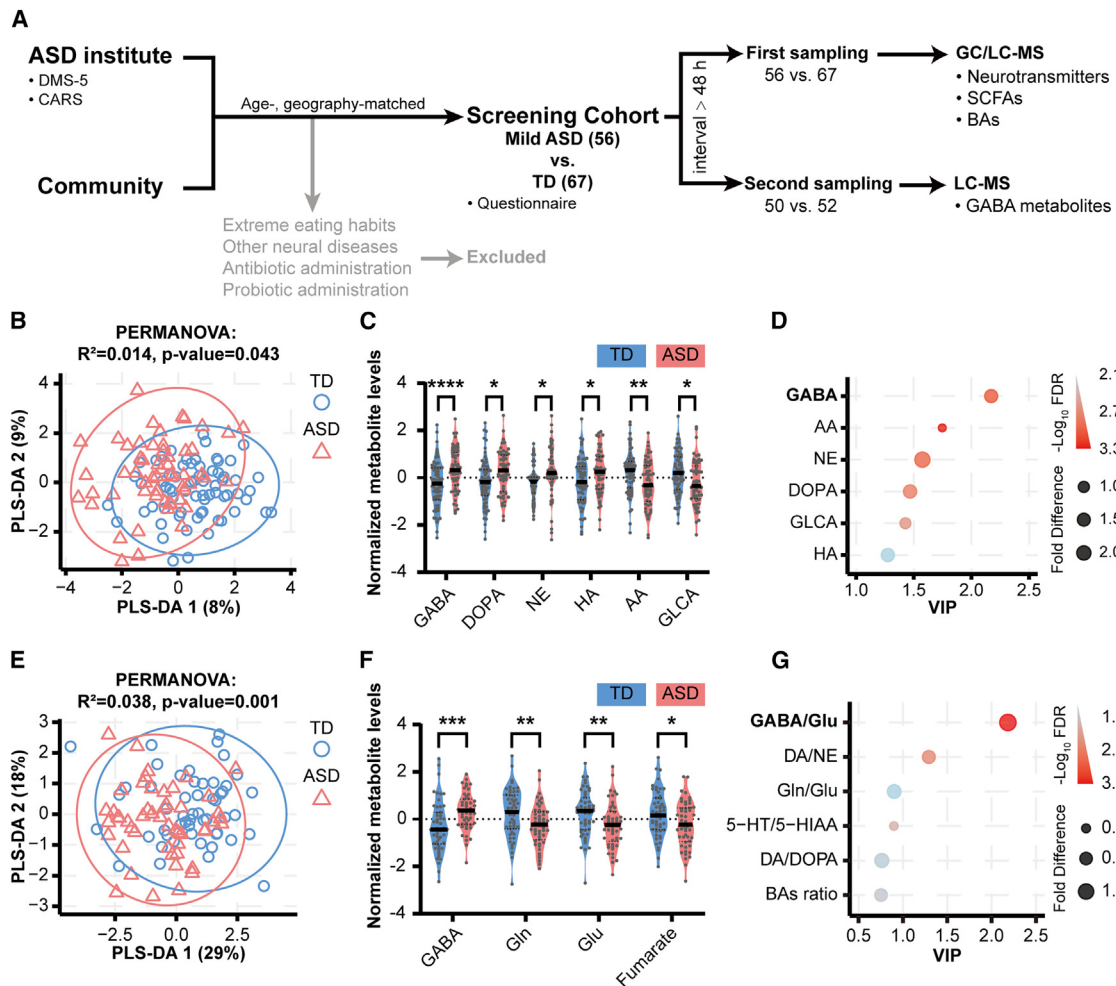
Figure 1. Imbalanced gut microbial GABA and Glu metabolism as an age- and gender-independent signature of ASD

(A) Workflow of experimental design for the screening cohort.

(B) Gut microbial metabolic profiling from the first sampling based on PLS-DA, revealing significant distinctions between the ASD ($n = 56$) and TD ($n = 67$) groups. PERMANOVA p value is shown.

(C) Significantly altered metabolites in the ASD group ($n = 56$) compared with the TD group ($n = 67$).

(D) GABA is identified as the most significantly changed metabolite among the differential metabolites.

(E) GABA-associated metabolic profiling from the second sampling based on PLS-DA plots, distinguishing between the ASD ($n = 50$) and TD ($n = 52$) groups. PERMANOVA p value is shown.

(F) Significantly altered GABA-associated metabolites in the ASD group ($n = 50$) compared with the TD group ($n = 52$).

(G) Indices representing specific metabolism balances compared between the ASD ($n = 56$) and TD ($n = 67$) groups.

In all violin plots, data are presented as metabolite INT data after adjusting confounders, and the horizontal line represents the median value in each group. Statistical significance: $^*p < 0.05$, $^{**}p < 0.01$, $^{***}p < 0.001$, and $^{****}p < 0.0001$; Student's t test.

Abbreviations: DSM-5, diagnostic and statistical manual of mental disorders, fifth edition; CARS, Childhood Autism Rating Scale; ASD, autism spectrum disorder; TD, typical development; GC, gas chromatography; LC, liquid chromatography; MS, mass spectrometry; SCFAs, short-chain fatty acids; BAs, bile acids; PLS-DA, partial least-squares discriminant analysis; VIP, variable importance for the projection; GABA, γ-aminobutyric acid; DOPA, dihydroxyphenylalanine; HA, histidine; NE, noradrenaline; GLCA, glycolithocholic acid; AA, acetic acid; Glu, glutamate; Gln, glutamine; INT, inverse normal transformation; PERMANOVA, permutational multivariate analysis of variance.

we also computed various ratios representing multiple metabolic pathways using the same datasets, including dopamine to norepinephrine or dihydroxyphenylalanine in tyrosine metabolism, serotonin to 5-hydroxyindole-3-acetic acid in tryptophan metabolism, and secondary to primary BAs in BA metabolism. Upon comparing all these ratios between ASD and TD groups, we identified the GABA/Glu ratio as the sole potential biomarker for ASD

(Figure 1G). This is particularly noteworthy as GABA and Glu are the primary inhibitory and excitatory neurotransmitters in the nervous system, and their imbalance is known to trigger neuropsychiatric disorders.[31] Thus, the observed imbalance in gut microbial GABA metabolism, evidenced by an elevated GABA/Glu ratio, presents a distinctive metabolic signature of ASD that is independent of age and gender.

Microbial GABA/Glu ratio as an independent indicator for ASD diagnosis

To validate the ASD-specific metabolic alterations identified in our initial screening and to enhance geographical diversity of the study population, we established a new, geographically distinct cohort, referred to as the validating cohort (Figure 2A). Logistic regression analysis in this cohort indicated that gender and the consumption of specific foods, such as fruits, vegetables, dark vegetables, fungi, and algae, emerged as significant confounders associated with ASD diagnosis in this cohort (Figure 2B).

We then conducted metabolomics analysis with a focus on neurotransmitter metabolites, detecting a total of 21 metabolites, including GABA, Glu, and Gln (Table S3). To control for potential confounders such as geography, age, gender, and dietary habits, we applied the INT method to normalize metabolite levels. PLS-DA plots revealed distinct metabolomic profiles between the ASD and TD groups (Figure 2C). Notably, the ASD group consistently exhibited elevated levels of both GABA and the GABA/Glu ratio (Figure 2D), corroborating findings from the screening phase.

Furthermore, to assess the clinical diagnostic utility of the microbial GABA/Glu ratio for ASD, we performed a receiver operating characteristic analysis. The GABA/Glu ratio demonstrated strong diagnostic potential with an area under the curve of 0.759 (Figure 2E). Collectively, these results indicate that the microbial GABA/Glu ratio is a reliable and independent biomarker for ASD diagnosis.

Elevated GABA/Glu ratio linked to ASD-associated GM dysbiosis characterized by increased *Escherichia/ Shigella* abundance

To ferret out the underlying differences in GM composition between individuals with ASD and TD, alongside alterations in microbial GABA metabolism, we applied 16S rRNA gene sequencing on fecal samples from the screening cohort (Figure 3A). Using relative abundances of the bacterial taxa, we conducted both β-diversity and α-diversity analyses. Principal coordinates analysis based on β-diversity analysis delineated distinct GM profiles in the ASD group compared to the TD group (Figure 3B). However, in α-diversity analysis, both the Chao index (indicative of community richness) and the Shannon index (indicative of community diversity) showed comparable levels between the two groups (Figure 3C).

Subsequently, to identify specific bacterial genera associated with ASD, we harnessed Microbiome Multivariable Association with Linear Models 2 (MaAsLin2)[32] and linear discriminant analysis effect size (LEfSe) tool. Adjusting for age and gender, MaAsLin2 revealed 10 genera significantly associated with ASD diagnosis (Figure 3D; Table S4). LEfSe, which operates independently of confounders, identified 26 differentially abundant genera between the ASD and TD groups (Figure S1B). Notably, both methods consistently determined several genera, including *Escherichia/ Shigella*, *Megamonas*, *Megasphaera*, *Sarcina*, *Allisonella*, *Weissella*, and *Veillonella*, as significantly associated with ASD. These findings, in keeping with previous reports,[10,33] support the presence of distinct microbial community alterations in individuals with ASD.

Next, we investigated the potential link between GM dysbiosis and the imbalanced GABA metabolism. We assessed the aforementioned 7 differential genera between the ASD and TD groups using Pearson correlation analysis. After adjusting for age and gender, we identified two genera significantly correlated with the GABA/Glu ratio, including *Escherichia/ Shigella* and *Megasphaera* (Figure 3E). Intriguingly, among these, *Escherichia/Shigella* is the only known genus capable of producing GABA in the human gut,[34] implying that the elevated GABA/Glu ratio may be biologically linked to the over-representation of *Escherichia* or *Shigella* in individuals with ASD.

Considering individual variability in fecal samples, which may obscure the *bona fide* traits of GM dysbiosis in ASD, we hypothesized that a deteriorated GABA/Glu metabolic imbalance might render such dysbiotic features more evident. Consequently, we divided subjects with ASD into quartiles based on the GABA/Glu ratio (25% = −0.34; 50% = 0.32; 75% = 1.05) relative to the baseline levels in TD counterparts, and then sought to draw out the concomitant changes in GM composition. This included evaluating the Chao and Shannon indices and the relative abundance of *Escherichia/Shigella* at play. Strikingly, individuals with ASD in the top quartile of the GABA/Glu ratio exhibited the most pronounced GM dysbiosis, with significantly elevated abundance of *Escherichia/Shigella* (Figure 3F). Together, these findings suggest that an imbalance in microbial GABA/Glu metabolism is closely associated with GM dysbiosis in ASD, particularly with the over-representation of *Escherichia/Shigella*.

Imbalanced GABA metabolism associated with overall hypofunction of the GM community in ASD

To elucidate the molecular mechanism underlying GM dysbiosis associated with imbalanced GABA metabolism, we conducted metagenomic analysis and pertinent quantitative polymerase chain reaction (qPCR) validation on fecal samples (Figure 4A). We selected a subset of 7 subjects with ASD with relatively high GABA/Glu ratios (hASD, mean GABA/Glu = 1.172 ± 0.523) and 8 age- and gender-matched subjects with TD with normal GABA/Glu ratios near baseline (nTD, mean GABA/Glu = −0.437 ± 0.697) from our screening cohort. A third round of fecal sampling was collected from these participants, who were all male and between the ages of 3 and 5 years (Figure 4A).

Subsequently, we compared the structural and functional traits of the GM between the two groups. Bacterial taxonomy analysis confirmed a distinct structural alteration (Figure 4B), alongside significant declines in both richness and diversity of GM in children with hASD compared to their neurotypical peers (Figure 4C). Strikingly, Kyoto Encyclopedia of Genes and Genomes pathway analysis revealed that multiple molecular pathways related to cellular metabolism and homeostasis exhibited significantly decreased abundances. Specifically, these signaling categories included protein processing, longevity regulation, the tricarboxylic acid (TCA) cycle, and the metabolism of Glu, aspartate, alanine, and histidine ($p < 0.05$, FDR < 0.1) (Figure 4D). These disruptions in energy and amino acid metabolism, proteostasis, survival, and growth suggest a compromised viability of the GM in hASD.

Given that the GM inhabits a dynamic environment with various extracellular stressors, such as oxidative stress, which influence microbial viability and community structure, we
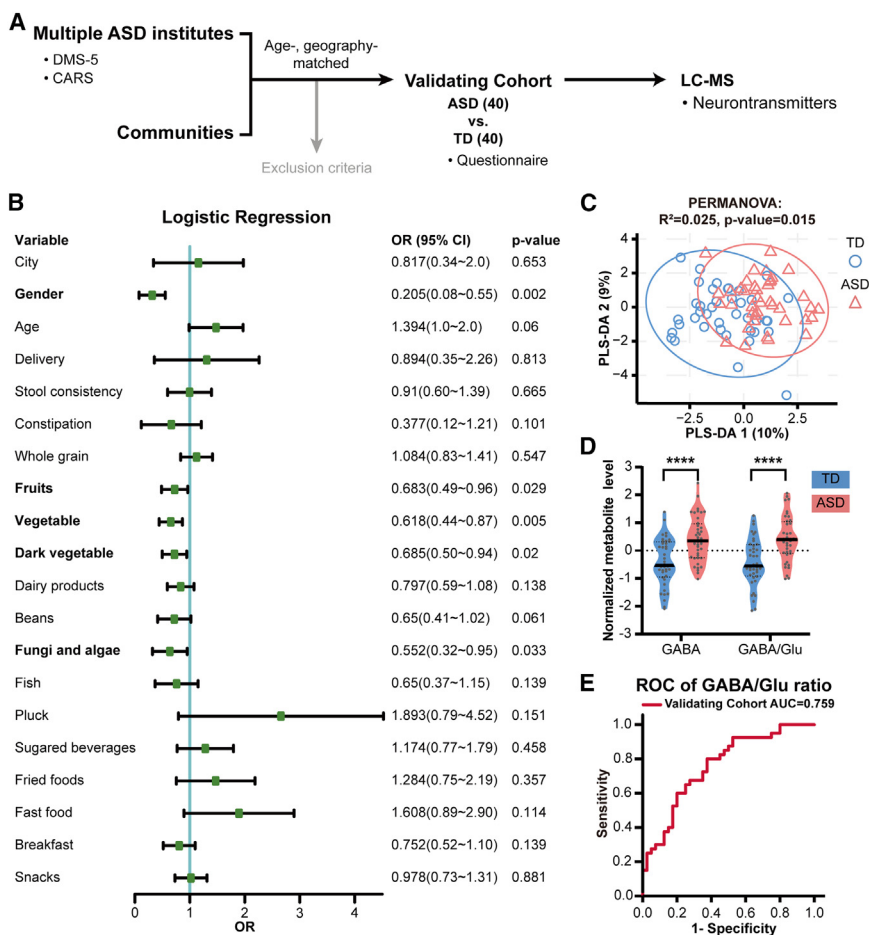
Figure 2. Gut microbial GABA/Glu ratio as an independent indicator associated with ASD diagnosis

(A) Workflow of experimental design for the validating cohort.

(B) Logistic regression identifies 5 confounders associated with ASD diagnosis in the validating cohort (ASD vs. TD = 40 vs. 40).

(C) Neurotransmitter profiling based on PLS-DA plots, revealing significant distinctions between the ASD ($n = 40$) and TD ($n = 40$) groups. PERMANOVA p value is shown.

(D) The validating cohort exhibits an increase in GABA and GABA/Glu ratio in the ASD group ($n = 40$) compared with the TD group ($n = 40$).

(E) ROC analysis demonstrates GABA/Glu ratio as a potent indicator for ASD diagnosis in the validating cohort.

In all violin plots, data are presented as metabolite INT data after adjusting confounders, and the horizontal line represents the median value in each group. Statistical significance: ****$p < 0.0001$; Student's t test.

Abbreviations: OR, odds ratio; ROC, receiver operating characteristic; AUC, area under the curve.

compared the abundances of several stress-response genes between the two groups. Our analysis revealed a significant increase in the abundance of genes like *gor*, *gpx*, *sod1*, and *katG* in the hASD group (Figure S2, abundance; Table S5). These genes encode enzymes involved in detoxifying superoxide and hydrogen peroxide, key intracellular processes triggered under extracellular stress conditions.[35–37] This increase in stress-response gene expression suggests an overload of oxidative stress in the GM, potentially reflecting an impaired intestinal environment. To further investigate the link between these stress-related changes and GABA metabolism, we performed a Pearson correlation analysis between the GABA/Glu ratio and the stress-response gene abundances. Notably, we observed significant correlations between the stress-response genes and the GABA/Glu ratio (Figure S2, coefficient), suggesting that aberrant GABA metabolism may indicate a stressed and dysfunctional GM community.

Among the identified ASD-associated pathways, the category of Glu, aspartate, and alanine metabolism comprised a series of enzyme-encoding genes involved in GABA metabolism regulation, such as *gabT* (GABA aminotransferase) and *gabD* (succinate semialdehyde dehydrogenase) for GABA degradation, as well as *gltD* (Glu synthase) and *purF* (amidophosphoribosyltransferase) for the synthesis of Glu and Gln, respectively. To further

reveal the molecular basis of the imbalanced GABA metabolism in ASD-linked GM, we analyzed the abundances of these genes (Figure 4E, (1) abundance). We found significant increases in *gabT* and *gabD*, concomitant with significant decreases in *gltD* and *purF* in hASD relative to nTD. Given that the transcription of *gabT* and *gabD* is GABA dependent in microbes, such as species of *Escherichia* and *Bacillus*,[38,39] our results suggests that adequate supplies of microbial GABA ensure GABA consumption in the GM community of individuals with ASD. Furthermore, other genes involved in metabolic interactions among Glu, aspartate, and alanine, including *aspB*, *argG*, *asdA*, and *ala*, consistently declined in hASD. Further, Pearson correlation analysis revealed that most of these aforementioned genes were significantly correlated with the GABA/Glu ratio after adjusting for age and gender (Figure 4E, (1) coefficient). These molecular-level results are consistent with our metabolomic findings of an increased GABA/Glu ratio, confirming that the microbial GABA metabolism was disrupted in individuals with ASD.

Overrepresentation of *Escherichia* possibly contributed to the aberrant GABA metabolism in ASD

To better understand the role of *Escherichia* in GABA metabolism, we mapped the metagenomics results against the Virulence Factor Database, which includes known bacterial factors involved in the colonization of host intestinal epithelium, microbe-host communication, and reciprocal responses. We identified a panel of 21 available *E. coli*-specific adhesins known to facilitate bacterial colonization of the intestinal epithelium.[40] By comparing the abundances of these adhesins between the
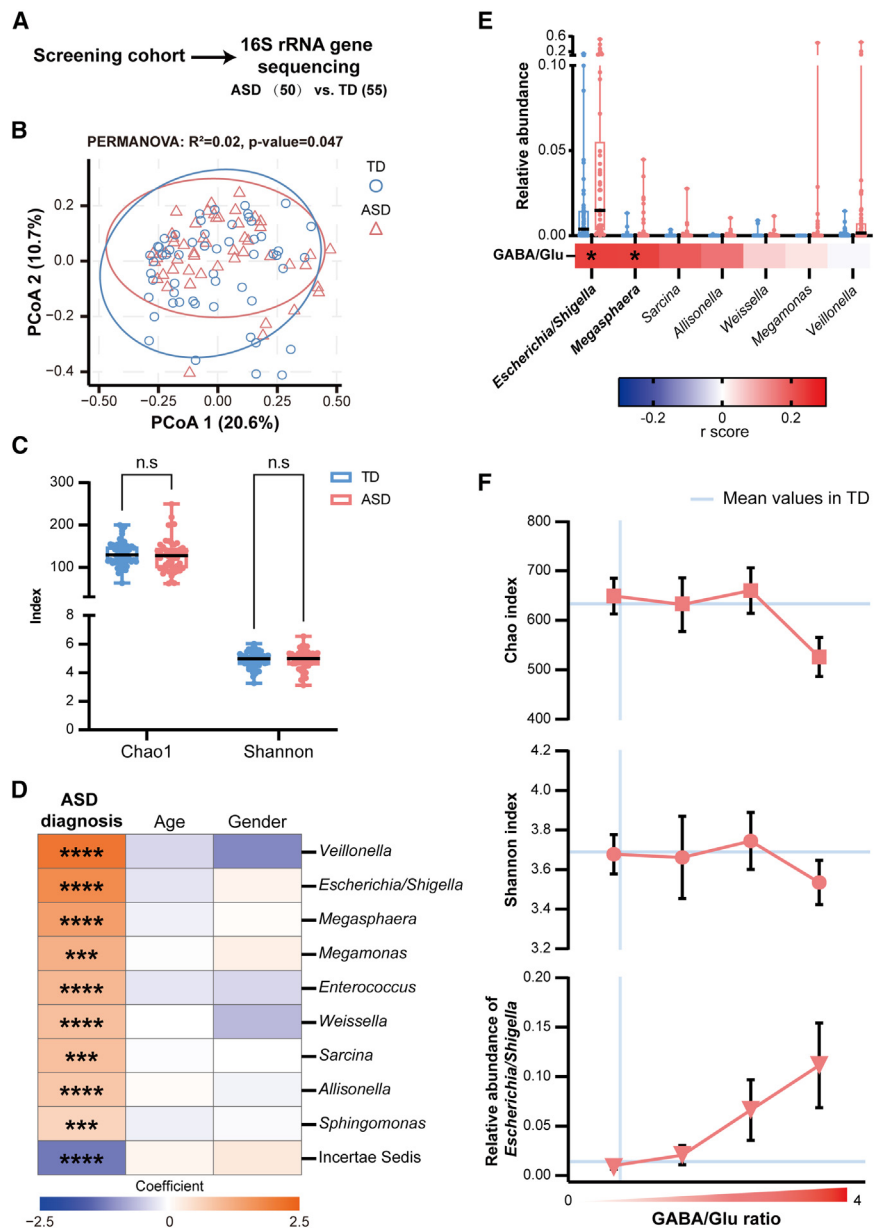
Figure 3. Elevated GABA/Glu ratio is associated with altered structural dysbiosis of GM in ASD

(A) Workflow depicting samples from the screening cohort utilized for 16S rRNA sequencing.

(B) PCoA plots based on microbial β-diversity, illustrating significant distinctions in the gut microbial component between the ASD ($n = 50$) and TD ($n = 55$) groups. PERMANOVA p value is shown.

(C) Microbial α-diversity analysis indicates comparable Chao and Shannon indices between the ASD ($n = 50$) and TD ($n = 55$) groups.

(D) MaAsLin2 analysis identifies 10 GM genera significantly associated with ASD diagnosis after adjusting age and gender (ASD vs. TD = 50 vs. 55). ***$p < 0.001$ and ****$p < 0.0001$; MaAsLin2.

(E) Boxplots depict the relative abundances of GABA/Glu ratio-associated genera (top). Heatmap displays the Pearson correlation (r score) between GM genera and GABA/Glu ratio (bottom). *$p < 0.05$; Pearson correlation analysis.

(F) Indices of Chao and Shannon, along with the relative abundance of *Escherichia/Shigella*, in each quartile of autistic subjects categorized based on their GABA/Glu ratio.

In all boxplots, the horizontal line represents the median value, and the whiskers extend from the minimum to the maximum values in each group. Wilcoxon rank-sum test is used in boxplots.

Abbreviations: PCoA, principal coordinates analysis; MaAsLin, microbiome multivariable association with linear models; GM, gut microbiome.

hASD was consistently higher than in nTD controls, whereas the relative abundance of *Shigella* remained very low in both groups (Figure 4F). To consolidate that *Escherichia* could contribute to GABA production, we examined the key enzymes involved in the microbial GABA-producing pathway through qPCR, focusing on the genus-specific glutamate decarboxylase (GAD) genes, *gadA* and *gadB*. Both genes showed significantly increased abundances in *Escherichia* (Figure 4G).
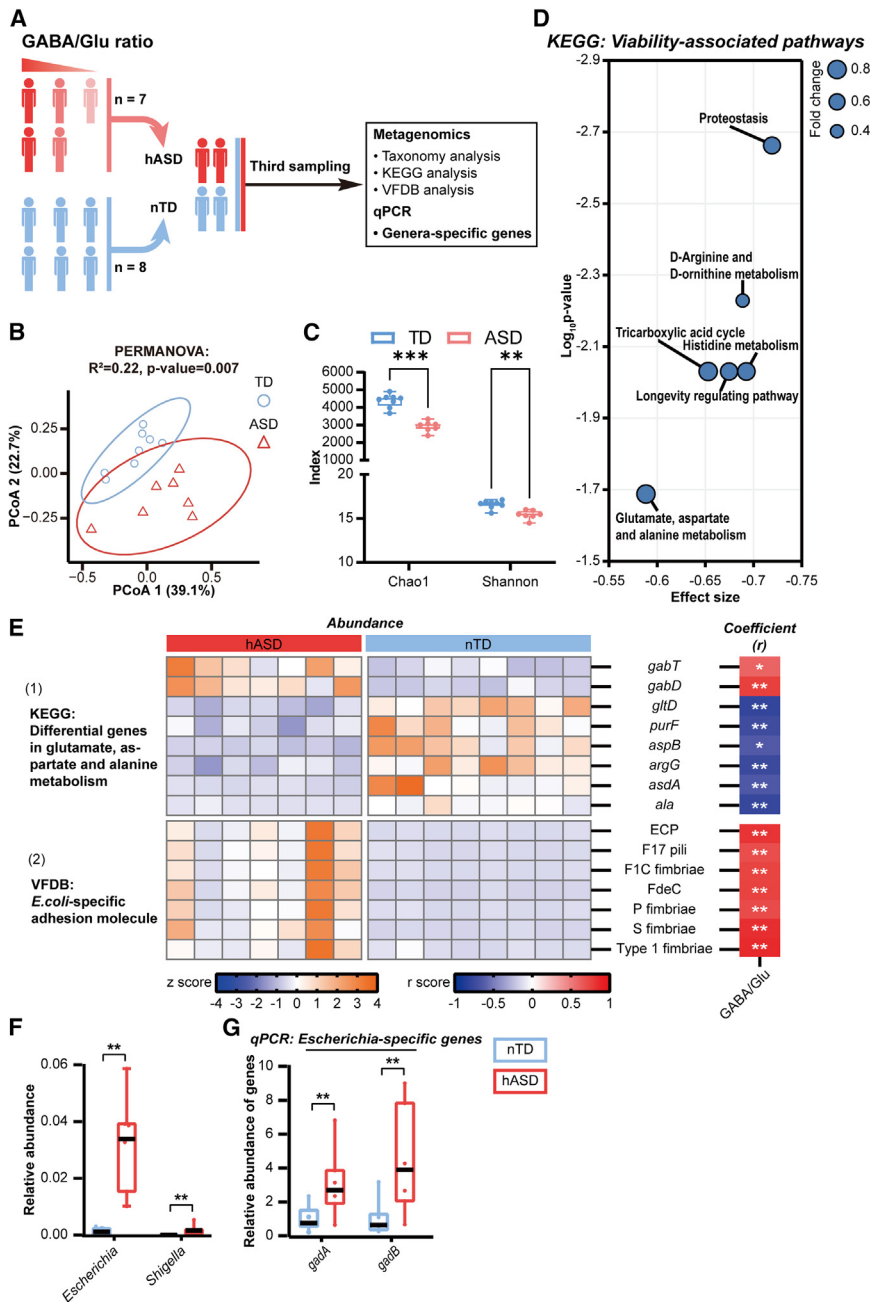
hASD and nTD groups, we determined that 7 molecules, such as P fimbriae, S fimbriae, and F1C fimbriae, were significantly increased in the hASD group (Figure 4E, (2) abundance). Notably, the abundances of each of these molecules were significantly associated with the GABA/Glu ratio after adjusting for age and gender (Figure 4E, (2) coefficient), implying that microbial GABA/Glu ratio was influenced by the colonization status of *Escherichia* species. The remaining adhesins exhibited an ascending trend in abundance, though not statistically significant (Table S6).

To establish a potential *Escherichia*-GABA axis, we analyzed the relative abundances of the genera *Escherichia* and *Shigella*, which could not be distinguished individually by 16S rRNA gene sequencing. The abundance of *Escherichia* in subjects with

Taken together, these findings suggest that overrepresentation of *Escherichia* may give rise to excess GABA via the *gad* genes, thereby contributing to the elevated GABA/Glu ratio in children with ASD.

Bacterial challenge with *E. coli* elicited social deficits in mice associated with altered GABA metabolism

To elucidate the impact of GM dysbiosis, characterized by overrepresentation of *Escherichia*, on host behavior, we conducted an *E. coli* challenge experiment on male C57BL6/J mice. To investigate the GABA production by *E. coli in vitro*, we first tested the capacity of a commercial non-pathogenic *E. coli* strain to produce GABA from Glu. We genetically engineered the *E. coli* strain to knock out either *gadA*, *gadB*, or both genes

Figure 4. GABA/Glu imbalance is associated with excessive GABA production and overgrown *Escherichia* in ASD

(A) Autistic subjects with relatively high GABA/Glu ratio (hASD) and age-, gender-matched subjects with TD with normal GABA/Glu ratio (nTD) are selected from the screening cohort for metagenomics and qPCR.

(B and C) Compared to the nTD group ($n = 8$), the hASD group ($n = 7$) shows (B) distinguished GM structure (PERMANOVA p value is shown) with (C) significantly decreased Chao and Shannon indices.

(D) KEGG analysis shows a significant decline in abundances of multiple viability-associated pathways in the hASD group ($n = 7$) compared with the nTD group ($n = 8$).

(E) (1) GABA-metabolism-associated genes identified by KEGG analysis and their association with the GABA/Glu ratio; (2) *E. coli*-specific adhesins identified by VFDB analysis and their association with the GABA/Glu ratio. $*p < 0.05$, $**p < 0.01$; Pearson correlation analysis.

(F) Overrepresented *Escherichia* and *Shigella* in the hASD group ($n = 7$) compared with the nTD group ($n = 8$).

(G) qPCR results demonstrate that gene abundances of *Escherichia*-specific *gadA* and *gadB* are significantly increased in the hASD group ($n = 7$) compared with the nTD group ($n = 8$).

In all boxplots, the horizontal line represents the median value, and the whiskers extend from the minimum to the maximum values in each group. Statistical significance: $**p < 0.01$ and $***p < 0.001$; Wilcoxon rank-sum test.

Abbreviations: KEGG, Kyoto Encyclopedia of Genes and Genomes; VFDB, Virulence Factor Database.

crease in the abundance of *E. coli* (Figure 5D) and the *Escherichia*-specific *gad* genes (Figure 5E) resulting from the *E. coli* challenge.

Furthermore, the three-chamber test (Figure 5F) revealed normal social preference (Figure 5G) but a significant deficit in social recognition (Figure 5H) in the *E. coli*-challenged group, suggesting a substantial reduction in social activity caused by the *E. coli* transplantation.

(Figure 5A). Subsequently, we measured the GABA levels of the wild-type and knockout strains using a GABA assay kit. Our results showed that the knockout strains exhibited significantly reduced GABA levels compared to the wild-type strain (Figure 5B), confirming the *gad*-dependent GABA production by *E. coli*.

In the subsequent *in vivo* experiments, wild-type *E. coli* was administered intragastrically from post-natal days 21 to 25 (P21–P25) to mimic the situation of *Escherichia* overgrowth in preschoolers (Figure 5C). After a 7-day colonization period, qPCR of fecal microbiome DNA demonstrated a substantial in-

Supporting this, subsequent tests of reciprocal social interaction (Figure 5I) depicted that the time spent interacting with a stranger mouse was significantly decreased in the *E. coli*-challenged group (Figure 5J).
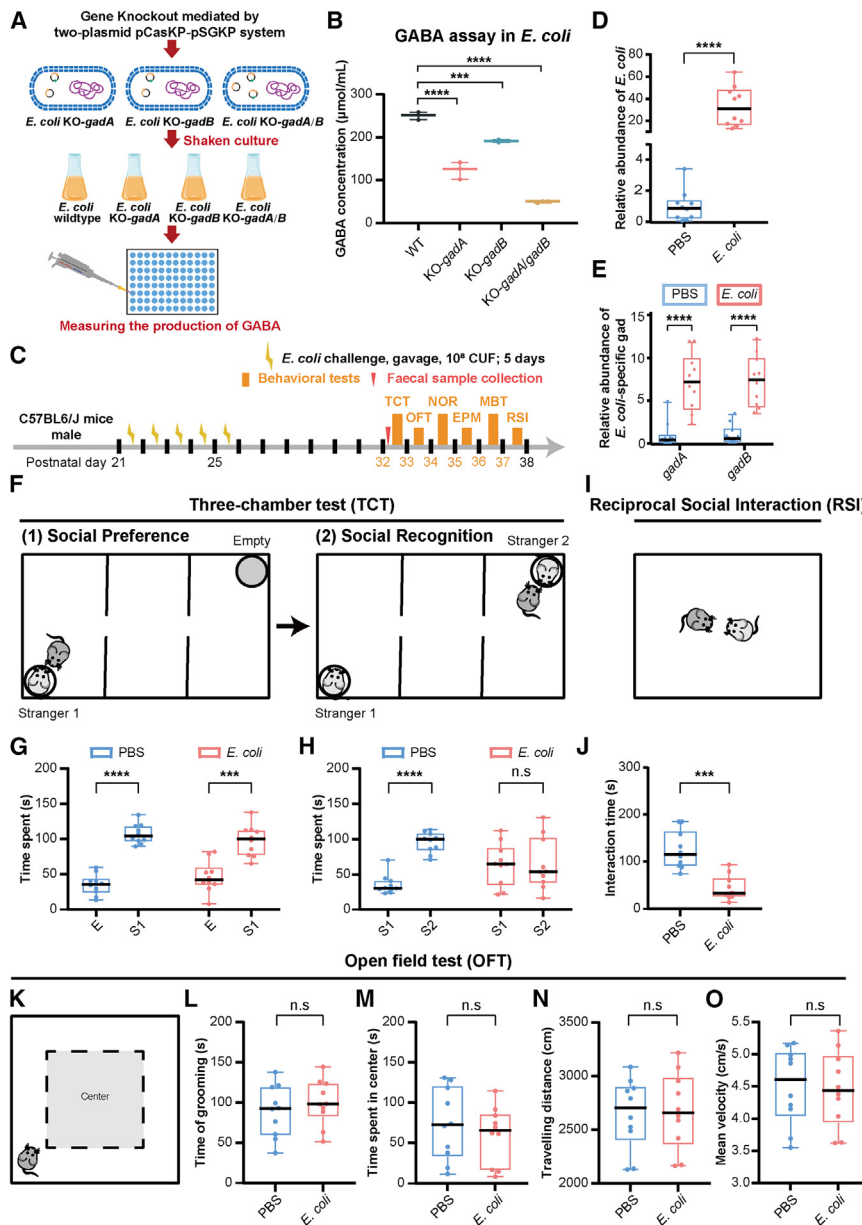
In the open field test (Figure 5K), grooming times were comparable between the two groups (Figure 5L), suggesting no repetitive behavior in the *E. coli*-challenged group, as also observed in the marble-burying test (Figure S3A). Comparisons of time spent in the center (Figure 5M), traveling distance (Figure 5N), and mean velocity (Figure 5O) showed no significant differences between the two groups. In addition, other behaviors, including

Figure 5. Challenge of *E. coli* in the gut leads to social deficiencies in mice

(A) Experimental workflow for *in vitro* assays: genetic modification of *E. coli* and GABA quantification.

(B) Comparative analysis of GABA levels in culture media of wild-type ($n = 3$), KO-*gadA* ($n = 3$), KO-*gadB* ($n = 3$), and KO-*gadA/gadB* ($n = 3$) *E. coli* strains.

(C) *In vivo* experimental schema: administration of wild-type *E. coli* strain in mice followed by a series of behavioral assessments. Comparative analyses are conducted between the *E. coli*-challenged group ($n = 10$) and the PBS group ($n = 10$).

(D and E) The *E. coli*-challenged group shows significantly increased relative abundances of (D) gut *E. coli* and (E) *E. coli*-specific *gad* compared to the PBS group.

(F) Diagram of three-chamber test (TCT).

(G and H) The *E. coli*-challenged group shows (G) normal social preference and (H) deficits in social recognition.

(I) Diagram of reciprocal social interaction (RSI).

(J) The *E. coli*-challenged group shows significantly decreased sniffing time with a stranger mouse compared to the PBS group.

(K) Diagram of open field test (OFT).

(L–O) The *E. coli*-challenged group shows comparable (L) time of grooming, (M) time spent in the center, (N) traveling distance, and (O) mean velocity to the PBS group.

In all boxplots, the horizontal line represents the median value, and the whiskers extend from the minimum to the maximum values in each group. Statistical significance: $***p < 0.01$ and $****p < 0.001$; Wilcoxon rank-sum test.

Abbreviations: PBS, phosphate-buffered saline; NOR, novel object recognition task; EPM, elevated plus maze; MBT, marble-burying test; CFU, colony-forming unit.

novel object recognition (Figure S3B) and elevated plus maze (Figure S3C), remained unchanged in the *E. coli*-challenged group. These findings indicate a specific role of *E. coli* in regulating social behaviors, independent of anxiety, recognition memory abnormalities, or alterations in locomotor activity.

DISCUSSION

Our findings of an elevated microbial GABA/Glu ratio in children with mild ASD are partially supported by previous metabolomics studies, which reported increased levels of carboxyethyl GABA[10] and decreased α-ketoglutarate,[22] respectively. These compounds are intermediate metabolites in the synthesis of GABA and Glu, respectively. We also noted that some studies have

otherwise observed lower fecal GABA levels in individuals with ASD, although these findings lacked statistical significance.[41,42] These discrepancies could arise from confounding factors, smaller sample size, or inconsistent participant stratification. In this study, we strengthened our analytical rigor by employing two distinct cohorts: a geographically unified screening cohort and a geographically diverse validating cohort. Remarkably, both cohorts consistently demonstrated elevated levels of GABA and increased GABA/Glu ratios in preschool-aged children with ASD. This reproducibility across different demographic contexts enhances the reliability of our results and validates the robustness of our metabolomic approach. Additionally, multiple studies, including our own, have highlighted the reduced activity of Glu metabolism-associated pathways as critical indicators of microbial functional changes in ASD, particularly in children around the age of four.[22,23,43,44] By integrating our genetic pathway analysis with metabolomic verification, we further demonstrated an increased GABA supply and a reduction in Glu

synthesis within the ASD-linked GM community. These findings collectively suggest that imbalanced GABA metabolism is a distinguishing feature of GM in children with mild ASD.

We observed an overall reduction in GM functionality, here termed hypofunction, in autistic subjects with an imbalanced GABA/Glu metabolism. This aligns with growing evidence pointing to a suboptimal, inefficient state of ASD-linked GM, including impaired detoxifying ability, decreased neurotransmitter synthesis, and delayed microbiota maturity.[10,21–23,45] GABA plays a central role in carbon and nitrogen metabolism, as its degradation through the TCA cycle contributes essential carbon atoms for cellular metabolism,[34] while its synthesis from Gln and Glu regulates ammonia homeostasis.[46] Accordingly, GABA accumulation could reflect a TCA cycle blockade within a compromised GM community, and an imbalance in GABA/Glu metabolism may disrupt ammonia homeostasis, potentially inducing oxidative stress.[47] This is supported by our finding of enriched stress-response genes in the ASD-linked GM. Moreover, our findings in the GM may also mirror metabolic processes in the brain, as a recent study has highlighted a potential parallel between the microbiome and brain metabolism in patients with ASD.[15] Previous studies have shown that cerebral GABA metabolism is implicated in the modulation of oxidative stress in the brain,[48–50] particularly in regions like the cerebellum and frontal and temporal lobes,[51] serving as a hallmark in children with ASD.[52,53] Therefore, GABA may act as a functional link between the gut microbiome and brain function. Animal studies have shown that changes in the GM alterations can affect GABA levels in both the bloodstream and the brain,[54,55] suggesting that shifts in microbial GABA metabolism may have systemic and neurological consequences in ASD.

Our results, in line with previous studies, indicate an increased abundance of the genus *Escherichia* in individuals with ASD. Strati et al. reported a link between constipation and distinct bacterial profiles in autistic and neurotypical subjects, with constipated autistic individuals exhibiting high levels of *Escherichia/Shigella*.[33] Although not the primary focus of their work, Dan et al. reported elevated abundance of *Escherichia/Shigella* in both the non-constipated ASD group and the overall ASD group compared to the TD controls.[10] More recently, a large-scale clinical study reported an early-life increase in *Escherichia* abundance in subjects with ASD,[56] aligning with the age range of our cohorts. These consistent observations across studies underscore the potential significance of *Escherichia* in ASD. Our investigation extends these findings by linking the *Escherichia* overrepresentation to disrupted GABA metabolism. The conversion of Glu to GABA in *Escherichia* species is known to facilitate adaptation to acidic environment,[57] like the intestinal tract. Indeed, we found that specific adhesins associated with *E. coli* were positively correlated with the GABA/Glu ratio, indicating an adaptive metabolic response by *Escherichia* during intestinal colonization. This link is further supported by findings of significantly elevated *Escherichia*-specific *gadA* and *gadB* abundance in both children with ASD and *E. coli*-challenged mice. We also investigated potential relationships between other known GABA producers (e.g., *Bacteroides*, *Parabacteroides*, *Bifidobacterium*, and *Lactobacillus*)[34,58] and GABA metabolism in our ASD cohort. However, these genera were either reduced or

unchanged in subjects with ASD and showed no significant association with the fecal GABA/Glu ratio (Figure S3A). Additionally, the *Bacteroides*-specific *gad* gene exhibited a decreasing tendency (Figure S3B).

We established an *E. coli* transplantation experiment in weaning mice to simulate an *Escherichia*-enriched GM community similar to that observed in preschoolers with ASD. Notably, the behavioral phenotype of this mouse model is similar to that observed in mice with a global deficit of the *chd8* gene,[59] one of the major genetic risk factors associated with ASD. Our findings suggest that postnatal factors, such as an *Escherichia*-enriched GM and aberrant GABA metabolism, may play significant roles in modulating social behaviors. This has important implications, as targeting gut microbial contributors is likely more feasible with current medical interventions, especially when correcting genomic mutations remains challenging.

We observed a reduced intake of fiber-rich foods, such as fruits, vegetables, fungi, and algae, among children with ASD. This is notable given prior research indicated that low-fiber diets can promote the overrepresentation of potentially pathogenic bacterial genera, including *Enterobacteriaceae*, *Escherichia/Shigella*, and *Clostridium XIVa*.[60] Consistent with these findings, our results demonstrate an increased abundance of *Escherichia/Shigella* in children with ASD, suggesting that dietary practices may contribute to GM dysbiosis. Furthermore, we unveiled a link between *Escherichia* overrepresentation and aberrant GABA metabolism. Metabolites central to the GABA metabolism pathway, such as GABA and succinate, are well recognized for their influence on host appetite and food preferences.[61] This aligns with prior studies that connect altered GABA metabolism with atypical feeding behaviors, including diminished post-weaning feeding, hyperphagia, and heightened hunger-induced appetite.[61] Collectively, these findings suggest a bidirectional relationship in children with ASD, where the host's physiological state not only shapes dietary preferences but is also reciprocally influenced by changes in GM composition. This intricate interplay between diet, microbiota composition, and GABA metabolism may contribute to the complex etiology of ASD and underscores the potential of microbiota-targeted interventions in managing ASD-related symptoms.

Limitations of the study

Firstly, the sample sizes in our clinical ASD cohorts were relatively modest. This limitation is shared across much of ASD-related microbiome research globally, where sample sizes often range from dozens to a few hundred participants, largely due to challenges in consistent recruitment and the high costs associated with sequencing. We employed a two-phase study design: an initial comprehensive screening to delineate the metabolite-microbiome axis, followed by a validation phase to confirm the reproducibility of our findings. To enhance the representativeness of our ASD cohort in future work, a meta-analysis incorporating published studies and publicly available datasets could be valuable. Secondly, although *Escherichia* species are conceptually known as GABA producers, we have yet to elucidate the explicit mechanisms underlying the relationship between gut *Escherichia* and the GABA metabolism within the entire GM community, which is worth in-depth investigations in the future.

Lastly, while our preliminary findings suggest that *E. coli* transplantation influences social behavior in animal models, additional research is needed to elucidate these effects. Our conclusions are based on a limited range of behavioral tests, and broader testing would provide a more comprehensive assessment of the role of *E. coli* in social behavior regulation.

RESOURCE AVAILABILITY

Lead contact
Further information and requests for resources and reagents should be directed to and will be fulfilled by the lead contact, Ningning Li (linn29@mail.sysu.edu.cn).

Materials availability
This study did not generate new unique reagents.

Data and code availability
- Raw data from genomic sequencing and metabolomics have been deposited at NCBI's Sequence Read Archive and MetaboLights, respectively. Data are publicly available as of the date of publication. Accession numbers are listed in the key resources table.
- This paper does not report original code.
- Any additional information required to reanalyze the data reported in this work is available from the lead contact upon request.

AUTHOR CONTRIBUTIONS

Study design, D.W., N.L., Huiliang Li, Y.P., and Y.H.; participant recruitment and sampling, D.W., Y.J., J.J., N.L., X.F., L.L., Hai Li, Z.D., S.F., and Y.H.; metabolomics and genomics, bioinformatics analysis, and animal experiments, D.W., Y.J., J.J., Y.P., Y.Y., and X.S.Z.; experimental data analysis, D.W., Y.J., J.J., N.L., Huiliang Li, and Y.P.; writing and revising, D.W., Y.J., J.J., N.L., Huiliang Li, Y.H., D.M., and X.S.Z.; supervision, N.L. All authors have read and approved the published version of the manuscript.

DECLARATION OF INTERESTS

The authors declare no competing interests.

STAR★METHODS

Detailed methods are provided in the online version of this paper and include the following:

SUPPLEMENTAL INFORMATION

Supplemental information can be found online at https://doi.org/10.1016/j.xcrm.2024.101919.

REFERENCES

1. Mottron, L., and Bzdok, D. (2020). Autism spectrum heterogeneity: fact or artifact? Mol. Psychiatr. *25*, 3178–3185. https://doi.org/10.1038/s41380-020-0748-y.

2. Lai, M.C., Lombardo, M.V., and Baron-Cohen, S. (2014). Autism. Lancet (London, England) *383*, 896–910. https://doi.org/10.1016/s0140-6736(13)61539-1.

3. Zwaigenbaum, L., Bauman, M.L., Choueiri, R., Kasari, C., Carter, A., Granpeesheh, D., Mailloux, Z., Smith Roley, S., Wagner, S., Fein, D., et al. (2015). Early Intervention for Children With Autism Spectrum Disorder Under 3 Years of Age: Recommendations for Practice and Research. Pediatrics *136*, S60–S81. https://doi.org/10.1542/peds.2014-3667E.

4. Constantino, J.N., and Charman, T. (2016). Diagnosis of autism spectrum disorder: reconciling the syndrome, its diverse origins, and variation in expression. Lancet Neurol. *15*, 279–291. https://doi.org/10.1016/s1474-4422(15)00151-9.

5. Sorboni, S.G., Moghaddam, H.S., Jafarzadeh-Esfehani, R., and Soleimanpour, S. (2022). A Comprehensive Review on the Role of the Gut Microbiome in Human Neurological Disorders. Clin. Microbiol. Rev. *35*, e0033820. https://doi.org/10.1128/cmr.00338-20.

6. Cryan, J.F., O'Riordan, K.J., Sandhu, K., Peterson, V., and Dinan, T.G. (2020). The gut microbiome in neurological disorders. Lancet Neurol. *19*, 179–194. https://doi.org/10.1016/s1474-4422(19)30356-4.

7. Kang, D.W., Adams, J.B., Gregory, A.C., Borody, T., Chittick, L., Fasano, A., Khoruts, A., Geis, E., Maldonado, J., McDonough-Means, S., et al. (2017). Microbiota Transfer Therapy alters gut ecosystem and improves gastrointestinal and autism symptoms: an open-label study. Microbiome 5, 10. https://doi.org/10.1186/s40168-016-0225-7.

8. Kang, D.W., Adams, J.B., Coleman, D.M., Pollard, E.L., Maldonado, J., McDonough-Means, S., Caporaso, J.G., and Krajmalnik-Brown, R. (2019). Long-term benefit of Microbiota Transfer Therapy on autism symptoms and gut microbiota. Sci. Rep. 9, 5821. https://doi.org/10.1038/s41598-019-42183-0.

9. Liu, F., Li, J., Wu, F., Zheng, H., Peng, Q., and Zhou, H. (2019). Altered composition and function of intestinal microbiota in autism spectrum disorders: a systematic review. Transl. Psychiatry 9, 43. https://doi.org/10.1038/s41398-019-0389-6.

10. Dan, Z., Mao, X., Liu, Q., Guo, M., Zhuang, Y., Liu, Z., Chen, K., Chen, J., Xu, R., Tang, J., et al. (2020). Altered gut microbial profile is associated with abnormal metabolism activity of Autism Spectrum Disorder. Gut Microb. 11, 1246–1267. https://doi.org/10.1080/19490976.2020.1747329.

11. Chen, Y.C., Lin, H.Y., Chien, Y., Tung, Y.H., Ni, Y.H., and Gau, S.S.F. (2022). Altered gut microbiota correlates with behavioral problems but not gastrointestinal symptoms in individuals with autism. Brain Behav. Immun. 106, 161–178. https://doi.org/10.1016/j.bbi.2022.08.015.

12. Yap, C.X., Henders, A.K., Alvares, G.A., Wood, D.L.A., Krause, L., Tyson, G.W., Restuadi, R., Wallace, L., McLaren, T., Hansell, N.K., et al. (2021). Autism-related dietary preferences mediate autism-gut microbiome associations. Cell 184, 5916–5931.e17. https://doi.org/10.1016/j.cell.2021.10.015.

13. Solden, L.M., Naas, A.E., Roux, S., Daly, R.A., Collins, W.B., Nicora, C.D., Purvine, S.O., Hoyt, D.W., Schückel, J., Jørgensen, B., et al. (2018). Interspecies cross-feeding orchestrates carbon degradation in the rumen ecosystem. Nat. Microbiol. 3, 1274–1284. https://doi.org/10.1038/s41564-018-0225-4.

14. Manor, O., Levy, R., and Borenstein, E. (2014). Mapping the inner workings of the microbiome: genomic- and metagenomic-based study of metabolism and metabolic interactions in the human microbiome. Cell Metabol. 20, 742–752. https://doi.org/10.1016/j.cmet.2014.07.021.

15. Morton, J.T., Jin, D.M., Mills, R.H., Shao, Y., Rahman, G., McDonald, D., Zhu, Q., Balaban, M., Jiang, Y., Cantrell, K., et al. (2023). Multi-level analysis of the gut-brain axis shows autism spectrum disorder-associated molecular and microbial profiles. Nat. Neurosci. 26, 1208–1217. https://doi.org/10.1038/s41593-023-01361-0.

16. Sherwin, E., Bordenstein, S.R., Quinn, J.L., Dinan, T.G., and Cryan, J.F. (2019). Microbiota and the social brain. Science 366, eaar2016. https://doi.org/10.1126/science.aar2016.

17. Paudel, R., Raj, K., Gupta, Y.K., and Singh, S. (2020). Oxiracetam and Zinc Ameliorates Autism-Like Symptoms in Propionic Acid Model of Rats. Neurotox. Res. 37, 815–826. https://doi.org/10.1007/s12640-020-00169-1.

18. Jiang, J., Wang, D., Jiang, Y., Yang, X., Sun, R., Chang, J., Zhu, W., Yao, P., Song, K., Chang, S., et al. (2024). The gut metabolite indole-3-propionic acid activates ERK1 to restore social function and hippocampal inhibitory synaptic transmission in a 16p11.2 microdeletion mouse model. Microbiome 12, 66. https://doi.org/10.1186/s40168-024-01755-7.

19. Wang, T., Chen, B., Luo, M., Xie, L., Lu, M., Lu, X., Zhang, S., Wei, L., Zhou, X., Yao, B., et al. (2023). Microbiota-indole 3-propionic acid-brain axis mediates abnormal synaptic pruning of hippocampal microglia and susceptibility to ASD in IUGR offspring. Microbiome 11, 245. https://doi.org/10.1186/s40168-023-01656-1.

20. Averina, O.V., Kovtun, A.S., Polyakova, S.I., Savilova, A.M., Rebrikov, D.V., and Danilenko, V.N. (2020). The bacterial neurometabolic signature of the gut microbiota of young children with autism spectrum disorders. J. Med. Microbiol. 69, 558–571. https://doi.org/10.1099/jmm.0.001178.

21. Wan, Y., Zuo, T., Xu, Z., Zhang, F., Zhan, H., Chan, D., Leung, T.F., Yeoh, Y.K., Chan, F.K.L., Chan, R., and Ng, S.C. (2022). Underdevelopment of the gut microbiota and bacteria species as non-invasive markers of pre-

diction in children with autism spectrum disorder. Gut 71, 910–918. https://doi.org/10.1136/gutjnl-2020-324015.

22. Wang, M., Wan, J., Rong, H., He, F., Wang, H., Zhou, J., Cai, C., Wang, Y., Xu, R., Yin, Z., and Zhou, W. (2019). Alterations in Gut Glutamate Metabolism Associated with Changes in Gut Microbiota Composition in Children with Autism Spectrum Disorder. mSystems 4, e00321-18. https://doi.org/10.1128/mSystems.00321-18.

23. Zhang, M., Chu, Y., Meng, Q., Ding, R., Shi, X., Wang, Z., He, Y., Zhang, J., Liu, J., Zhang, J., et al. (2020). A quasi-paired cohort strategy reveals the impaired detoxifying function of microbes in the gut of autistic children. Sci. Adv. 6, eaba3760. https://doi.org/10.1126/sciadv.aba3760.

24. Zuckerman, K.E., Friedman, N.D.B., Chavez, A.E., Shui, A.M., and Kuhlthau, K.A. (2017). Parent-Reported Severity and Health/Educational Services Use Among US Children with Autism: Results from a National Survey. J. Dev. Behav. Pediatr. 38, 260–268. https://doi.org/10.1097/dbp.0000000000000437.

25. Kadwa, R.A., Sahu, J.K., Singhi, P., Malhi, P., and Mittal, B.R. (2019). Prevalence and Characteristics of Sensory Processing Abnormalities and its Correlation with FDG-PET Findings in Children with Autism. Indian J. Pediatr. 86, 1036–1042. https://doi.org/10.1007/s12098-019-03061-9.

26. Morales Hidalgo, P., Voltas Moreso, N., and Canals Sans, J. (2021). Autism spectrum disorder prevalence and associated sociodemographic factors in the school population: EPINED study. Autism 25, 1999–2011. https://doi.org/10.1177/13623613211007717.

27. Zhang, R., Yu, X., Yu, Y., Guo, D., He, H., Zhao, Y., and Zhu, W. (2022). Family Food Environments and Their Association with Primary and Secondary Students' Food Consumption in Beijing, China: A Cross-Sectional Study. Nutrients 14, 1970. https://doi.org/10.3390/nu14091970.

28. Underwood, J.M., Brener, N., Thornton, J., Harris, W.A., Bryan, L.N., Shanklin, S.L., Deputy, N., Roberts, A.M., Queen, B., Chyen, D., et al. (2020). Overview and Methods for the Youth Risk Behavior Surveillance System - United States, 2019. MMWR Suppl. 69, 1–10. https://doi.org/10.15585/mmwr.su6901a1.

29. Oh, D., and Cheon, K.A. (2020). Alteration of Gut Microbiota in Autism Spectrum Disorder: An Overview. Soa Chongsonyon Chongsin Uihak. 31, 131–145. https://doi.org/10.5765/jkacap.190039.

30. Pain, O., Dudbridge, F., and Ronald, A. (2018). Are your covariates under control? How normalization can re-introduce covariate effects. Eur. J. Hum. Genet. 26, 1194–1201. https://doi.org/10.1038/s41431-018-0159-6.

31. Basu, S.K., Pradhan, S., du Plessis, A.J., Ben-Ari, Y., and Limperopoulos, C. (2021). GABA and glutamate in the preterm neonatal brain: In-vivo measurement by magnetic resonance spectroscopy. Neuroimage 238, 118215. https://doi.org/10.1016/j.neuroimage.2021.118215.

32. Mallick, H., Rahnavard, A., McIver, L.J., Ma, S., Zhang, Y., Nguyen, L.H., Tickle, T.L., Weingart, G., Ren, B., Schwager, E.H., et al. (2021). Multivariable association discovery in population-scale meta-omics studies. PLoS Comput. Biol. 17, e1009442. https://doi.org/10.1371/journal.pcbi.1009442.

33. Strati, F., Cavalieri, D., Albanese, D., De Felice, C., Donati, C., Hayek, J., Jousson, O., Leoncini, S., Renzi, D., Calabrò, A., and De Filippo, C. (2017). New evidences on the altered gut microbiota in autism spectrum disorders. Microbiome 5, 24. https://doi.org/10.1186/s40168-017-0242-1.

34. Strandwitz, P., Kim, K.H., Terekhova, D., Liu, J.K., Sharma, A., Levering, J., McDonald, D., Dietrich, D., Ramadhar, T.R., Lekbua, A., et al. (2019). GABA-modulating bacteria of the human gut microbiota. Nat. Microbiol. 4, 396–403. https://doi.org/10.1038/s41564-018-0307-3.

35. Yang, L., Mih, N., Anand, A., Park, J.H., Tan, J., Yurkovich, J.T., Monk, J.M., Lloyd, C.J., Sandberg, T.E., Seo, S.W., et al. (2019). Cellular responses to reactive oxygen species are predicted from molecular mechanisms. Proc. Natl. Acad. Sci. USA 116, 14368–14373. https://doi.org/10.1073/pnas.1905039116.

36. Eisenhardt, K.M.H., Remes, B., Grützner, J., Spanka, D.T., Jäger, A., and Klug, G. (2021). A Complex Network of Sigma Factors and sRNA StsR Regulates Stress Responses in R. sphaeroides. Int. J. Mol. Sci. 22, 7557. https://doi.org/10.3390/ijms22147557.

37. Yura, T. (2019). Regulation of the heat shock response in Escherichia coli: history and perspectives. Genes Genet. Syst. 94, 103–108. https://doi.org/10.1266/ggs.19-00005.

38. Peng, Q., Yang, M., Wang, W., Han, L., Wang, G., Wang, P., Zhang, J., and Song, F. (2014). Activation of gab cluster transcription in Bacillus thuringiensis by γ-aminobutyric acid or succinic semialdehyde is mediated by the Sigma 54-dependent transcriptional activator GabR. BMC Microbiol. 14, 306. https://doi.org/10.1186/s12866-014-0306-3.

39. Okuda, K., Kato, S., Ito, T., Shiraki, S., Kawase, Y., Goto, M., Kawashima, S., Hemmi, H., Fukada, H., and Yoshimura, T. (2015). Role of the amino-transferase domain in Bacillus subtilis GabR, a pyridoxal 5'-phosphate-dependent transcriptional regulator. Mol. Microbiol. 95, 245–257. https://doi.org/10.1111/mmi.12861.

40. Klemm, P. (1985). Fimbrial adhesions of Escherichia coli. Rev. Infect. Dis. 7, 321–340. https://doi.org/10.1093/clinids/7.3.321.

41. De Angelis, M., Piccolo, M., Vannini, L., Siragusa, S., De Giacomo, A., Serrazzanetti, D.I., Cristofori, F., Guerzoni, M.E., Gobbetti, M., and Francavilla, R. (2013). Fecal microbiota and metabolome of children with autism and pervasive developmental disorder not otherwise specified. PLoS One 8, e76993. https://doi.org/10.1371/journal.pone.0076993.

42. Kang, D.W., Ilhan, Z.E., Isern, N.G., Hoyt, D.W., Howsmon, D.P., Shaffer, M., Lozupone, C.A., Hahn, J., Adams, J.B., and Krajmalnik-Brown, R. (2018). Differences in fecal microbial metabolites and microbiota of children with autism spectrum disorders. Anaerobe 49, 121–131. https://doi.org/10.1016/j.anaerobe.2017.12.007.

43. Chen, T., Chen, C., Wu, H., Chen, X., Xie, R., Wang, F., Sun, H., and Chen, L. (2021). Overexpression of p53 accelerates puberty in high-fat diet–fed mice through Lin28/let-7 system. Exp. Biol. Med. 246, 66–71. https://doi.org/10.1177/1535370220961320.

44. Heberling, C., and Dhurjati, P. (2015). Novel systems modeling methodology in comparative microbial metabolomics: identifying key enzymes and metabolites implicated in autism spectrum disorders. Int. J. Mol. Sci. 16, 8949–8967. https://doi.org/10.3390/ijms16048949.

45. Needham, B.D., Adame, M.D., Serena, G., Rose, D.R., Preston, G.M., Conrad, M.C., Campbell, A.S., Donabedian, D.H., Fasano, A., Ashwood, P., and Mazmanian, S.K. (2021). Plasma and Fecal Metabolite Profiles in Autism Spectrum Disorder. Biol. Psychiatr. 89, 451–462. https://doi.org/10.1016/j.biopsych.2020.09.025.

46. Dalangin, R., Kim, A., and Campbell, R.E. (2020). The Role of Amino Acids in Neurotransmission and Fluorescent Tools for Their Detection. Int. J. Mol. Sci. 21, 6197. https://doi.org/10.3390/ijms21176197.

47. Norenberg, M.D. (2003). Oxidative and nitrosative stress in ammonia neurotoxicity. Hepatology (Baltimore, Md 37, 245–248. https://doi.org/10.1053/jhep.2003.50087.

48. Beltrán González, A.N., López Pazos, M.I., and Calvo, D.J. (2020). Reactive Oxygen Species in the Regulation of the GABA Mediated Inhibitory Neurotransmission. Neuroscience 439, 137–145. https://doi.org/10.1016/j.neuroscience.2019.05.064.

49. Abruzzo, P.M., Panisi, C., and Marini, M. (2021). The Alteration of Chloride Homeostasis/GABAergic Signaling in Brain Disorders: Could Oxidative Stress Play a Role? Antioxidants 10, 1316. https://doi.org/10.3390/antiox10081316.

50. Hou, C.W. (2011). Pu-Erh tea and GABA attenuates oxidative stress in kainic acid-induced status epilepticus. J. Biomed. Sci. 18, 75. https://doi.org/10.1186/1423-0127-18-75.

51. Chauhan, A., Gu, F., Essa, M.M., Wegiel, J., Kaur, K., Brown, W.T., and Chauhan, V. (2011). Brain region-specific deficit in mitochondrial electron transport chain complexes in children with autism. J. Neurochem. 117, 209–220. https://doi.org/10.1111/j.1471-4159.2011.07189.x.

52. James, S.J., Cutler, P., Melnyk, S., Jernigan, S., Janak, L., Gaylor, D.W., and Neubrander, J.A. (2004). Metabolic biomarkers of increased oxidative stress and impaired methylation capacity in children with autism. Am. J. Clin. Nutr. 80, 1611–1617. https://doi.org/10.1093/ajcn/80.6.1611.

53. Wang, J., Fröhlich, H., Torres, F.B., Silva, R.L., Poschet, G., Agarwal, A., and Rappold, G.A. (2022). Mitochondrial dysfunction and oxidative stress contribute to cognitive and motor impairment in FOXP1 syndrome. Proc. Natl. Acad. Sci. USA 119, 66–71. https://doi.org/10.1073/pnas.2112852119.

54. Matsumoto, M., Ooga, T., Kibe, R., Aiba, Y., Koga, Y., and Benno, Y. (2017). Colonic Absorption of Low-Molecular-Weight Metabolites Influenced by the Intestinal Microbiome: A Pilot Study. PLoS One 12, e0169207. https://doi.org/10.1371/journal.pone.0169207.

55. Hassan, A.M., Mancano, G., Kashofer, K., Fröhlich, E.E., Matak, A., Mayerhofer, R., Reichmann, F., Olivares, M., Neyrinck, A.M., Delzenne, N.M., et al. (2019). High-fat diet induces depression-like behaviour in mice associated with changes in microbiome, neuropeptide Y, and brain metabolome. Nutr. Neurosci. 22, 877–893. https://doi.org/10.1080/1028415X.2018.1465713.

56. Lou, M., Cao, A., Jin, C., Mi, K., Xiong, X., Zeng, Z., Pan, X., Qie, J., Qiu, S., Niu, Y., et al. (2022). Deviated and early unsustainable stunted development of gut microbiota in children with autism spectrum disorder. Gut 71, 1588–1599. https://doi.org/10.1136/gutjnl-2021-325115.

57. Richard, H.T., and Foster, J.W. (2003). Acid resistance in Escherichia coli. Adv. Appl. Microbiol. 52, 167–186. https://doi.org/10.1016/s0065-2164(03)01007-4.

58. Barrett, E., Ross, R.P., O'Toole, P.W., Fitzgerald, G.F., and Stanton, C. (2012). γ-Aminobutyric acid production by culturable bacteria from the human intestine. J. Appl. Microbiol. 113, 411–417. https://doi.org/10.1111/j.1365-2672.2012.05344.x.

59. Yu, Y., Zhang, B., Ji, P., Zuo, Z., Huang, Y., Wang, N., Liu, C., Liu, S.-J., and Zhao, F. (2022). Changes to gut amino acid transporters and microbiome associated with increased E/I ratio in Chd8+/- mouse model of ASD-like behavior. Nat. Commun. 13, 1151. https://doi.org/10.1038/s41467-022-28746-2.

60. Valenzuela-Zamora, A.F., Ramírez-Valenzuela, D.G., and Ramos-Jiménez, A. (2022). Food Selectivity and Its Implications Associated with Gastrointestinal Disorders in Children with Autism Spectrum Disorders. Nutrients 14, 2660. https://doi.org/10.3390/nu14132660.

61. Han, H., Yi, B., Zhong, R., Wang, M., Zhang, S., Ma, J., Yin, Y., Yin, J., Chen, L., and Zhang, H. (2021). From gut microbiota to host appetite: gut microbiota-derived metabolites as key regulators. Microbiome 9, 162. https://doi.org/10.1186/s40168-021-01093-y.

62. Wang, Y., Wang, S., Chen, W., Song, L., Zhang, Y., Shen, Z., Yu, F., Li, M., and Ji, Q. (2018). CRISPR-Cas9 and CRISPR-Assisted Cytidine Deaminase Enable Precise and Efficient Genome Editing in Klebsiella pneumoniae. Appl. Environ. Microbiol. 84, e01834-18. https://doi.org/10.1128/AEM.01834-18.

63. Bolyen, E., Rideout, J.R., Dillon, M.R., Bokulich, N.A., Abnet, C.C., Al-Ghalith, G.A., Alexander, H., Alm, E.J., Arumugam, M., Asnicar, F., et al. (2019). Reproducible, interactive, scalable and extensible microbiome data science using QIIME 2. Nat. Biotechnol. 37, 852–857. https://doi.org/10.1038/s41587-019-0209-9.

64. Callahan, B.J., McMurdie, P.J., Rosen, M.J., Han, A.W., Johnson, A.J.A., and Holmes, S.P. (2016). DADA2: High-resolution sample inference from Illumina amplicon data. Nat. Methods 13, 581–583. https://doi.org/10.1038/nmeth.3869.

65. Tang, S., Liu, W., Zhao, Q., Li, K., Zhu, J., Yao, W., and Gao, X. (2021). Combination of polysaccharides from Astragalus membranaceus and Codonopsis pilosula ameliorated mice colitis and underlying mechanisms. J. Ethnopharmacol. 264, 113280. https://doi.org/10.1016/j.jep.2020.113280.

66. Drewes, J.L., White, J.R., Dejea, C.M., Fathi, P., Iyadorai, T., Vadivelu, J., Roslani, A.C., Wick, E.C., Mongodin, E.F., Loke, M.F., et al. (2017).

High-resolution bacterial 16S rRNA gene profile meta-analysis and biofilm status reveal common colorectal cancer consortia. NPJ Biofilms Microbiomes *3*, 34. https://doi.org/10.1038/s41522-017-0040-3.

67. Bolger, A.M., Lohse, M., and Usadel, B. (2014). Trimmomatic: a flexible trimmer for Illumina sequence data. Bioinformatics *30*, 2114–2120. https://doi.org/10.1093/bioinformatics/btu170.

68. Price, M.N., Dehal, P.S., and Arkin, A.P. (2010). FastTree 2 – Approximately Maximum-Likelihood Trees for Large Alignments. PLoS One *5*, e9490. https://doi.org/10.1371/journal.pone.0009490.

69. Katoh, K., and Standley, D.M. (2013). MAFFT Multiple Sequence Alignment Software Version 7: Improvements in Performance and Usability. Mol. Biol. Evol. *30*, 772–780.

70. Bokulich, N.A., Kaehler, B.D., Rideout, J.R., Dillon, M., Bolyen, E., Knight, R., Huttley, G.A., and Gregory Caporaso, J. (2018). Optimizing taxonomic classification of marker-gene amplicon sequences with QIIME 2's q2-feature-classifier plugin. Microbiome *6*, 90. https://doi.org/10.1186/s40168-018-0470-z.

71. DeSantis, T.Z., Hugenholtz, P., Larsen, N., Rojas, M., Brodie, E.L., Keller, K., Huber, T., Dalevi, D., Hu, P., and Andersen, G.L. (2006). Greengenes, a chimera-checked 16S rRNA gene database and workbench compatible with ARB. Appl. Environ. Microbiol. *72*, 5069–5072. https://doi.org/10.1128/aem.03006-05.

72. Huijsdens, X.W., Linskens, R.K., Mak, M., Meuwissen, S.G.M., Vandenbroucke-Grauls, C.M.J.E., and Savelkoul, P.H.M. (2002). Quantification of bacteria adherent to gastrointestinal mucosa by real-time PCR. J. Clin. Microbiol. *40*, 4423–4427. https://doi.org/10.1128/jcm.40.12.4423-4427.2002.

73. Ju, J., Yang, X., Jiang, J., Wang, D., Zhang, Y., Zhao, X., Fang, X., Liao, H., Zheng, L., Li, S., et al. (2021). Structural and Lipidomic Alterations of Striatal Myelin in 16p11.2 Deletion Mouse Model of Autism Spectrum Disorder. Front. Cell. Neurosci. *15*, 718720. https://doi.org/10.3389/fncel.2021.718720.

74. Sgritta, M., Dooling, S.W., Buffington, S.A., Momin, E.N., Francis, M.B., Britton, R.A., and Costa-Mattioli, M. (2019). Mechanisms Underlying Microbial-Mediated Changes in Social Behavior in Mouse Models of Autism Spectrum Disorder. Neuron *101*, 246–259.e6. https://doi.org/10.1016/j.neuron.2018.11.018.

75. Xu, Z.X., Kim, G.H., Tan, J.W., Riso, A.E., Sun, Y., Xu, E.Y., Liao, G.Y., Xu, H., Lee, S.H., Do, N.Y., et al. (2020). Elevated protein synthesis in microglia causes autism-like synaptic and behavioral aberrations. Nat. Commun. *11*, 1797. https://doi.org/10.1038/s41467-020-15530-3.

76. Choleris, E., Thomas, A.W., Kavaliers, M., and Prato, F.S. (2001). A detailed ethological analysis of the mouse open field test: effects of diazepam, chlordiazepoxide and an extremely low frequency pulsed magnetic field. Neurosci. Biobehav. Rev. *25*, 235–260. https://doi.org/10.1016/s0149-7634(01)00011-2.

77. Leonzino, M., Ponzoni, L., Braida, D., Gigliucci, V., Busnelli, M., Ceresini, I., Duque-Wilckens, N., Nishimori, K., Trainor, B.C., Sala, M., and Chini, B. (2019). Impaired approach to novelty and striatal alterations in the oxytocin receptor deficient mouse model of autism. Horm. Behav. *114*, 104543. https://doi.org/10.1016/j.yhbeh.2019.06.007.

78. Buffington, S.A., Di Prisco, G.V., Auchtung, T.A., Ajami, N.J., Petrosino, J.F., and Costa-Mattioli, M. (2016). Microbial Reconstitution Reverses Maternal Diet-Induced Social and Synaptic Deficits in Offspring. Cell *165*, 1762–1775. https://doi.org/10.1016/j.cell.2016.06.001.

STAR★METHODS

KEY RESOURCES TABLE

REAGENT or RESOURCE	SOURCE	IDENTIFIER
Biological samples		
Stools from patients with autism spectrum disorder and typical development children	This paper	N/A
Deposited data		
16S RNA sequencing data	NCBI SRA	BioProject ID: PRJNA1046699
Metabolomics data	Metabolights	Metabolights ID: MTBLS11524, MTBLS11483
Experimental models: Organisms/strains		
E. coli	China Center of Industrial Culture Collection, China	CICC 20658
E. coli DH5α	Sangon Biotech	B528413
E. coli with KO-gadA	This paper	N/A
E. coli with KO-gadB	This paper	N/A
E. coli with KO-gadA/gadB	This paper	N/A
Oligonucleotides		
Primer: 16S rRNA (V3-V4) Forward primers: ACTCCTACGGGAGGCAGCAG	This paper	N/A
Primer: 16S rRNA (V3-V4) Reverse primers: GGACTACHVGGGTWTCTAAT	This paper	N/A
Primer: *Escherichia/Shigella-gadA* Forward primers: TAACGGATTTCCGCTCAGA	This paper	N/A
Primer: *Escherichia/Shigella-gadA* Reverse primers: TCGTTTTGACTCCGCGATAGTA	This paper	N/A
Primer: *Escherichia/Shigella-gadB* Forward primers: AACGGATTTAAGGTCGGAAC	This paper	N/A
Primer: *Escherichia/Shigella-gadB* Reverse primers: ACGTTTTGATTCTGCGATAGTG	This paper	N/A
Primer: *Bacteroides-gad* Forward primers: GTTCAGACAGAATGTTACAACCC	This paper	N/A
Primer: *Bacteroides-gad* Reverse primers: CATATAAGTGGTAACGAAAGTAGCC	This paper	N/A
Primer: *gadA* test-Forward primers: ATCAGGTAGGCAAAGAGCTG	This paper	N/A
Primer: *gadA* test-Reverse primers: GTCACCGCCATTAAAATAGCG	This paper	N/A
Primer: *gadB* test-Forward primers: GACTGAGCAGGAGCAATTGT	This paper	N/A
Primer: *gadB* test-Reverse primers: GTGAGCTGCTTAGCTTTACC	This paper	N/A
Primer: *gadA* ssDNA donor: TTTTATTGCCTT CAAATAAATTTAAGGAGTTCGAATAACATCA CGTTGTAAAAACCGAATGCCCAACCTT	This paper	N/A
Primer: *gadB* ssDNA donor: TTTTAATGCGAT CCAATCATTTTAAGGAGTTTAATAACGTTTA ACGGTAACGGTGTCCCGAAACGAAGC	This paper	N/A
Primer: sgRNA*gadA*-F1: TAGTAAAGGCCAT TTCTACTATCG	This paper	N/A
Primer: sgRNA*gadA*-R1: AAACCGATAGTA GAAATGGCCTTT	This paper	N/A

(Continued on next page)

Continued

REAGENT or RESOURCE	SOURCE	IDENTIFIER
Primer: sgRNA*gadB*-F1: TAGTGCAAGTAAC GGATTTAAGGT	This paper	N/A
Primer: sgRNA*gadB*-R1: AAACACCTTAAAT CCGTTACTTGC	This paper	N/A
Recombinant DNA		
Plasmid: pCasKP-apr	Wang et al.[62]	N/A
Plasmid: pSGKP-spe	Wang et al.[1]	N/A
Plasmid: pSGKP-*gadA*	This paper	N/A
Plasmid: pSGKP-*gadB*	This paper	N/A
Software and algorithms		
R (v3.6.3)	R statistical software	www.R-project.org/
SPSS (version 22)	IBM SPSS Statistics	N/A
QIIME 2.0	Bolyen et al.[63]	https://qiime2.org/
DADA 2.0	Callahan et al.[64]	https://benjjneb.github.io/dada2/
GraphPad Prism (v9)	GraphPad Software	N/A
SIMCA 14.1	SIMCA Software	N/A

EXPERIMENTAL MODEL AND STUDY PARTICIPANT DETAILS

Ethical statement
This human gut microbiota study was reviewed and approved by the Ethical Committee of The Seventh Affiliated Hospital of Sun Yat-sen University (No. 2018041901) and Sun Yat-sen Memorial Hospital (No. BAP20240677). Written informed consent was obtained from the guardians of the participants. Additionally, our animal study was reviewed and approved by the Animal Care and Use Committee of the Southern University of Science and Technology (Number: SUSTC-2019-155).

Human study design
Participant recruitment
Our study was systematically structured into two distinct phases: the screening phase and the validating phase. In the screening phase, children with ASD were recruited through ARK Autism & Rehabilitation Institute (Shanxi, China). In the validating phase, individuals with ASD were drawn from diverse sources, including ARK Autism & Rehabilitation Institute (Shanxi, China), Shenzhen Hospital (Guangdong, China), and Sun Yat-sen Memorial Hospital (Guangdong, China). Children with TD were included in the study from kindergartens and communities in proximity to the relevant ASD institutes. Inclusion criteria were set up as follows: 1) three to seventeen-year-old children with diagnosed ASD according to the Diagnostic and Statistical Manual of Mental Disorders, Fifth Edition (DSM-5) and age matched subjects with TD; 2) mild ASD cases assessed as per the CARS. In order to control for the associated biomedical and environmental confounders that may affect the subsequent analyses, exclusion criteria were set up as follows: 1) on unbalanced diets (completely refusing or extremely favoring specific staple foods); 2) diagnosed with severe ASD; 3) suffering from other neurologic or psychiatric disorders including epilepsy, schizophrenia, depression and attention-deficit/hyperactivity disorder; 4) suffering from intestinal infectious diseases; 5) antibiotic or probiotic administration within a month before sampling. To ensure temporal alignment, a questionnaire investigation was conducted with the enrolled children within two weeks preceding the stool sampling. Information on all participants, including age, gender, city, dietary habit, manner of birth, administration of drug/healthcare products and common pathological conditions (neurologic, psychiatric and gastrointestinal diseases), were gathered via questionnaire. Finally, two cohorts were recruited: a screening cohort (ASD vs. TD = 56 vs. 67) and a validating cohort (40 vs. 40) for autistic GM profiling screening and validation.

Fecal sampling principles and specimen consistency
To ensure high-quality samples, fecal sampling was conducted by the guardians of the research participants. They were trained in basic aseptic techniques, recognition of stool consistency, and the sampling procedure. First, assisted by their guardians, participants were all required to defecate on a prepared cellulose core diaper to separate feces from urine. Stool consistency of each excreta was then evaluated using the Bristol Stool Chart. Only corn-on-cob-like (type 3) or sausage-like (type 4) feces, indicative of normal stool, were sampled. Next, to avoid potential air-borne contamination, the surface part of the feces was not used. Instead, a sterile sampling scoop was used to withdraw the inner core of the stool. Finally, about 2 g of quality specimen were collected in a sterile collecting tube. These samples were refrigerated within 30 min of collection, and then handed over to one of our staff members for snap freezing and shipping by dry ice. For biological replicates, each participant's fecal sampling was performed two to three times, with a minimum interval of 48 h. The samples were aliquoted and stored at −80°C. They were later subjected to Ultra

Performance Liquid Chromatography with Tandem Mass Spectrometry (UPLC-MS/MS), Gas Chromatography-Mass Spectrometry (GC-MS), 16S rRNA gene sequencing, metagenomics or qPCR.

Sample grouping for multi-omics investigation

To mitigate analytical biases arising from random events during sampling, such as emotional fluctuations, subtle changes of daily diets, and weather variations, we utilized different sample sets from the screening cohort for multi-omics studies. The first sampling was dedicated to analyzing the metabolic and structural features of the GM and for screening distinct metabolites or taxa. The second and third samplings were employed for the functional analysis of changes in autistic GM. Samples from the validating cohort were specifically used to validate key findings.

Animal study design

Male C57BL/6J mice were housed in a pathogen-free facility under a 12-h light/12-h dark cycle. The 3-week-old male mice (P [post-natal day] 21) were randomly divided into an experimental group and a control group and then housed separately. Starting from P21, the experimental group was challenged with wild-type gut commensal *E. coli* by daily gavage at a dose of 10^8 per mouse for 5 consecutive days. Meanwhile, phosphate-buffered saline (PBS) was used as placebo in the control group. Subsequently, mice were housed for another 7 days for *E. coli* colonization. At P32, fecal samples from mice were collected and all mice were subjected to behavioral tests. The principles for mouse fecal sampling and storage were similar to those used in human studies. Each mouse was placed in an individual sterilized box for defecation. During sampling, any urine present was immediately wiped off with an anti-septic swab. Stool consistency was evaluated as previously described.[65] Accordingly, only hard-formed fecal stools, indicative of normal stool, were collected using sterilized tweezers and stored in tubes. Soft, unformed, or urine-contaminated samples were discarded.

METHOD DETAILS

Targeted metabolomics

In this study, a thorough metabolomics analysis was performed, which included two distinct rounds in the screening cohort and a subsequent validation round in the validating cohort. Initially, neurotransmitters, SCFAs, and BAs were analyzed using the first sampling from the screening cohort. Subsequently, the second sampling from this cohort was employed to investigate metabolites specifically associated with GABA metabolism. In the final phase, samples from the validating cohort were utilized to re-evaluate neurotransmitter levels, with the aim of confirming our key findings.

The analytical procedures employed in this study varied according to the metabolites being assessed. Neurotransmitters, BAs, and metabolites specific to GABA metabolism were analyzed using UPLC-MS/MS, while SCFAs were quantified via GC-MS. To ensure accuracy, isotope-labeled internal standards (ISs) were utilized for most measurements. However, for the neurotransmitter analysis in the screening cohort, external standards (ESs) were applied.

Quantification methodologies in this study varied depending on the type of standard used. For ISs, we calculated peak area ratios (PARs) by dividing the peak areas of the analytes by those of the ISs, enabling absolute quantification based on IS calibration curves. In contrast, when using ESs, the peak areas of the analytes were corrected relative to the ESs' peak areas, facilitating relative quantification. All standards employed in this study were sourced from Applied Protein Technology, Shanghai, China.

Sample preparation & extraction

To investigate the levels of different metabolite types, fecal samples were prepared using distinct methods. Neurotransmitter samples were prepared in pre-cooled acetonitrile containing 1% (v/v) formic acid (FA). Samples for BAs were added to pre-cooled methanol. For metabolites specific to GABA metabolism, samples were added to a pre-cooled solution of acetonitrile, methanol and water (2:2:1, v/v/v). After vortexing, these homogenates were incubated for 20 min at $-20°C$ to precipitate proteins, followed by centrifugation at 14,000 g for 15 min at $4°C$. The collected supernatants were then dried under vacuum. Next, the above sample extracts were in turn redissolved in solutions of acetonitrile in water (1:1, v/v), methanol in water (1:1, v/v), and acetonitrile and methanol in water (2:2:1, v/v/v), and centrifuged as described above. The supernatants were collected and subjected to UPLC-MS/MS. Fecal samples for assessing SCFAs were prepared in 15% (v/v) phosphoric acid, and subjected to GC-MS.

UPLC-MS/MS procedure

For neurotransmitters measurement, an Agilent 1290 Infinity UPLC system (Agilent, USA) equipped with an Acquity UPLC BEH C18 column (1.7 μm × 2.1 mm × 100 mm, Waters, Canada) was used to analyze the samples. The samples were put in an auto-sampler (chromatographic column temperature, $45°C$; flow velocity, 300 μL/min). The mobile phase consisted of 0.1% (v/v) ammonium formate (liquid A) and acetonitrile with 0.1% (v/v) FA (liquid B). A gradient-elution program was set as follows: starting from 90% B at 0 min, linear gradient was decreased to 40% B over 18 min; then eluent B was returned to 90% within 1 s and maintained for 5 min. Subsequently, an electrospray ionization (ESI)-triple 5500 quadrupole-linear ion trap (QTRAP)-mass spectrometer (AB SCIEX, USA) was applied to conduct mass spectrometry (MS) analysis in positive ion mode (ESI+). The ESI+ source conditions were as follows: ion spray voltage floating (ISVF), 5000 V; ion source gas1 (Gas1), 60; ion source gas2 (Gas2), 60; curtain gas (CUR), 30; source temperature, $450°C$.

For BAs measurement, a Waters Acquity UPLC I-Class system (Waters, USA) equipped with the Acquity UPLC BEH C18 column was used to analyze the samples. Samples were put in an auto-sampler (chromatographic column temperature, 45°C; flow velocity, 300 μL/min). The mobile phases were pure water with 0.1% (v/v) FA (liquid A) and methanol (liquid B). A gradient-elution program was set as follows: starting from 60% B at 0 min, linear gradient was increased to 65% B over 6 min and further to 80% B within 5 s; then, eluent B was returned to 90% within 1 s and maintained for 9 min. Subsequently, the 5500 QTRAP-mass spectrometer was applied to conduct MS analysis in negative ion mode (ESI -). The ESI - source conditions were as follows: ISVF, −4500 V; Gas1, 55; Gas2, 55; CUR, 40; source temperature, 550°C.

To measure metabolites specific to GABA metabolism, the Waters UPLC system was equipped with the same sampler using the same column conditions as described above for bile acids measurement. The mobile phases were pure water with 1.2% (v/v) ammonium (liquid A) and methanol with 0.2% (v/v) FA (liquid B). A gradient-elution program was set as follows: starting from 75% B at 0 min, linear gradient was first decreased to 62% B over 10 min and further to 40% B over the next 5 min; then, eluent B was returned to 75% within 30 s and held for 17 min. Subsequently, the 5500 QTRAP-mass spectrometer was applied to conduct MS analysis in both ESI+ and ESI- as described above.

Multiple Reaction Monitoring (MRM) was used for acquisition, detection, and quantification of metabolites in this study. Multi-Quant software (v3.0.2) was used to extract and correct the peak area and retention times from the chromatograms. The relative content of each corresponding metabolite was represented by the area of its respective peak.

GC-MS procedure

For SCFA analysis, an Agilent 6890N/5975B GC-MS spectrometer (Agilent, USA) was applied. Samples were added with 4-methylvaleric acid as an internal standard (83 ppm; Thermo Fisher Scientific), and put in an automatic sampler (carrier gas, helium; flow velocity, 1.0 mL/min; injection port temperature, 250°C; split injection, split ratio 10:1; solvent delay, 2.2 min) An HP-INNOWAX capillary GC column (30 m × 0.25 mm × 0.25 μm, Agilent) was used to separate the samples. Temperature programming was as follows: the initial temperature of the column oven was set at 90°C, and then increased to 120°C at a speed of 10°C/min, to 150°C at 5°C/min and finally to 250°C at 25°C/min, where it was held for 2 min. Subsequently, MS conditions were set as follows: electron bombardment ionization source; iron source temperature, 230°C; quadrupole temperature, 150°C; electron energy 70 eV.

Selected Ion Monitoring (SIM) mode was utilized for the detection of SCFAs. The MSD ChemStation software (v2.0) was used to extract and correct the peak area and retention time from the chromatograms. This allowed for the determination of the relative content of SCFAs, based on peak areas, and their identification, based on retention times.

Genomic analysis
Extraction of genomic DNA
Bacterial DNA was extracted from fecal stools using the QIAamp DNA Stool Mini Kit (QIAGEN, Germany) following the manufacturer's instructions. The presence and quality of genomic DNA were then assessed through 1% (w/v) agarose gel electrophoresis.
Bacterial 16S rRNA gene sequencing and annotation
The barcoded primers used to amplify the V3-V4 region of the 16S rRNA gene were 319F/806R.[66] The sequencing library was generated using the NEB NextUltraDNA Library Prep Kit for Illumina (NEB, USA), following the manufacturer's instructions. Sequencing was performed on an Illumina HiSeq2500 platform (Illumina, USA). QIIME (v2.0) served as the amplicon read processing pipeline (https://qiime2.org/).[63] Briefly, demultiplexed paired-end reads underwent initial trimming with Trimmomatic[67] to remove low-quality reads (Phred quality score <25, length <187 bp). These trimmed reads were then denoised with DADA2[64] to eliminate primer sequence (forward: 27 bp, reverse 30 bp). A phylogenetic tree was generated by FastTree,[68] following multiple sequence alignment and masking of highly variable positions using MAFFT.[69] Taxonomy was assigned using a pre-trained Naive Bayes classifier[70] based on the pre-created Greengene 13_8 99% identity OTUs.[71]
Metagenome sequencing and annotation
The sequencing library for metagenome sequencing was generated using the TruSeq DNA Sample Prep Kit (Illumina) following manufacturer. Paired-end sequencing was then performed on the Illumina HiSeq2500 platform. Host sequences were filtered out using BWA (http://bio-bwa.sourceforge.net) and remained reads were assembled with Megahit (https://github.com/voutcn/megahit). The annotations for taxonomy, functional pathway and bacterial virulence factors were performed with BLASTP (v2.2.31+). This process involved querying against the Non-Redundant Protein Sequence Database (https://ftp.ncbi.nlm.nih.gov/blast/db/FASTA/), KEGG (http://www.genome.jp/kegg/) and the VFDB (http://www.mgc.ac.cn/) respectively.

Quantification of glutamate decarboxylase in genera *Escherichia* and *Bacteroides*
Primers were designed against *Escherichia*- or *Bacteroides*-specific GAD DNA sequences obtained from the National Center of Biotechnology Information (NCBI). Two orthologs of *gad* in *Escherichia* were detected by *Escherichia-gadA*-qF/qR and *Escherichia-gadB*-qF/qR; *Bacteroides*-specific *gad* was detected by primer pair *Bacteroides-gad*-qF/qR. The qPCR reaction mixture for amplification consisted of 2 μL of Roche Fast Start LightCycler Mastermix, forward and reverse primers (0.5 mM each), 3.2 mM MgCl2 and nuclease-free water to a final volume of 15 μL. The amplification cycles consisted of incubation at 95°C for 30 s, at 57°C for 30 s, and 72°C for 30 s. Cycle threshold values were measured and target gene concentration was analyzed. Standard curve

generation, qPCR efficiency determination, and gene copy number calculation were performed using the 7500 Fast System SDS v1.4 software (Thermo Fisher Scientific).

Gene engineering in E. coli
Microbe strains
The gut commensal strain of *E. coli* (CICC20658) was purchased from the China Center of Industrial Culture Collection (CICC), China.

Materials and growth conditions
The bacterial strains, plasmids, and primers used in this study are detailed in the key resources table. *Escherichia coli* strains were cultured in Luria-Bertani (LB) medium with specific antibiotics at the following concentrations: 30 μg/mL apramycin and 100 μg/mL spectinomycin.

sgRNA design and plasmid construction
Subgenomic RNAs (sgRNAs), each with a 20-nucleotide (N20) base-pairing region, were designed using CRISPR sgRNA design software (http://blast.ncbi.nlm.nih.gov/Blast.cgi). Two sets of oligonucleotides (*gadA* test-F/*gadA* test-R *and gadB* test-F/*gadB* test-R) were ligated into the pSGKP-spe plasmid digested by BsaI and then transformed into *E. coli* DH5α competent cells.

Generation of *gadA* and *gadB* deletion mutants
Deletion Mutants: Nonpolar, markerless, in-frame deletions of *gadA* and *gadB* genes were generated using 70bp single-stranded DNA (ssDNA) repair templates via homologous recombination.[62] Electroporation and Selection: The pCasKP-apr plasmid was introduced into wild-type *E. coli*, with transformants selected using apramycin on LB agar plates. Co-electroporation and Cointegrants: The plasmids pSGKP-*gadA* and pSGKP-*gadB*, along with ssDNA, were co-electroporated into the pCasKP-harboring *E. coli* strain. Cointegrants were then selected on LB agar plates containing both apramycin and spectinomycin, which facilitated the selection due to genome double-strand breaks and subsequent homologous recombination. Colony qPCR Screening: Colony qPCR was used to identify clones carrying the mutant alleles. Double Mutants: To generate double mutants lacking either *gadA* or *gadB*, both plasmids were removed by incubating the bacteria at 37°C on sucrose plates, allowing colonies to emerge.

Preparation of electrocompetent cells
Wild-type *E. coli* cells were prepared for electroporation by initially growing them in an overnight culture. Similarly, *E. coli* cells harboring the pCasKP plasmid were prepared for electroporation, with the additional step of inducing these cells with L-arabinose.

Electroporation
The electrocompetent *E. coli* cells were mixed with either the plasmid or the donor template prior to electroporation. Following electroporation, the cells were allowed to recover and then plated on LB agar plates containing specific antibiotics. This selection step ensured the growth of only those cells that were successfully transformed.

Generation of dual *gadA/gadB* gene deletion mutants
To create mutants lacking the *gadA* gene, we employed a curing process on sucrose plates containing spectinomycin. The *gadB* deletion mutants were then generated using the same method as previously described.[62] This established method was adapted for the simultaneous deletion of both *gadA* and *gadB* genes, resulting in the creation of dual gene deletion mutants.

Assessment of GABA production in E. coli mutants
To evaluate GABA production in wild-type *E. coli* and its *gadA*, *gadB*, and dual *gadA/gadB* gene deletion mutants, we employed a GABA assay kit (Shanghai Enzyme-linked Biotechnology Co., Ltd., China). Briefly, bacterial cultures were grown using standard microbiological techniques. The cells were harvested and lysed, either through sonication or another suitable cell lysis method, to release intracellular components. For the GABA assay, we adhered to the kit's protocol, with minor modifications to suit our experimental needs. This included incubating the bacterial lysate in LB liquid medium enriched with glutathione at 37°C, with shaking at 220 rpm, and allowing the incubation to proceed overnight. GABA concentrations were quantified by measuring absorbance at 600 nm using a spectrophotometer and comparing the results to the standard curve provided with the kit.

Quantification of E. coli and Escherichia-specific glutamate decarboxylase
Primers targeting the 16S rDNA sequence of gut commensal *E. coli* were designed as previously described.[72] For quantifying *Escherichia*-specific *gadA* and *gadB*, we employed the same primers used in the human study. The qPCR procedure was conducted using the same methodology as described in the earlier section of this paper, ensuring consistency across both human and animal studies.

Behavioral tests on mice
Video recording during the behavioral tests were performed by EthoVision XT software (Noldus Information Technology, Leesburg, USA).

Three-chamber test

The social preference and social recognition abilities of mice were assessed using a three-chamber apparatus (60 × 40 × 20 cm, L x W x H) as previously described.[73,74] Briefly, the apparatus was divided into three interconnected chambers, with small cages placed in the left and right chambers, while the middle chamber remained empty. For habituation, the test mouse was first placed in the apparatus for 10 min. To evaluate social preference, the test mice were given the option to interact with an age- and gender-matched stranger mouse (Stranger 1) in the left chamber or to stay near the empty cage in the right chamber for the following 10 min. For social recognition assessment, a second stranger mouse (Stranger 2) was introduced into the previous empty cage in the right chamber for the final 10 min. The accumulative time that the test mouse spent in interacting with the empty cage, stranger 1 or stranger 2 was respectively recorded.

Marble-burying test

The repetitive behavior of mice was assessed in a mouse cage (42 × 24 × 12 cm, L x W x H) laid with 5 cm-thick corncob bedding as previously described.[75] Briefly, 20 glass beads (each 15 mm in diameter) were put into the cage and regularly divided into five rows (4 beads in each row). Then, the test mouse was placed in the cage for 30 min. The number of buried glass beads (being buried more than 50% of volume) was counted.

Open field test

Grooming, voluntary movement and anxiety behavior of mice were assessed in an open box (40 × 40 × 40 cm, L x W x H) as previously described.[73,76] Briefly, the open box was divided equally into 16 smaller grids and the central 4 grids were set as the central area (20 × 20 cm). Then, the test mouse was placed in the cage for 10 min. The grooming time of each mouse was recorded artificially. The speed, traveling distance and the time of each mouse that spent in the central area were calculated.

Novel object recognition

Recognition memory of mice was assessed in a box (40 × 40 × 40 cm, L x W x H) as previously described.[73,77] After 10-min habituation in the box, the test mouse was exposed to two identical objects for another 10 min. Then, one object was replaced with a novel object and the mouse was subsequently allowed to explore the objects for 10 min. The sniffing time at the proximity of each object within 2 cm or directly in touching the objects was recorded.

Elevated plus maze

The anxiety behavior of mice was assessed in a 1 m height platform consisting of 4 arms (two open arms and two closed arms crossed together) as previously described.[73] The test mouse was initially placed in the central area and their trails were recorded for 5 min. The accumulative time of the mouse in open arms and closed arms was calculated.

Reciprocal social interaction

As previously reported,[78] the test mouse was placed in a new cage and exposed to an age- and gender-matched stranger mouse for 10 min. The time of social interactions between the two mice (e.g., close following, touching, nose-to-nose sniffing, nose-to-anus sniffing, and crawling over/under each other) was calculated.

QUANTIFICATION AND STATISTICAL ANALYSIS

Statistical analyses were performed using R statistical software (v4.4.1) (www.R-project.org/) and SPSS (v22).

Confounders determination

Wilcoxon rank-sum test and Chi-square test were used to compare the average of continuous variables and frequency of nominal variable, respectively, between ASD and TD, with $p < 0.05$ as significant. Logistic regression was exploited to test the association between covariates and ASD diagnosis, with $p < 0.05$ as significant.

Metabolism profiling

INT upon levels and ratios of metabolites was performed to achieve normally distributed data after adjusting for confounders. Student's t test was used to compare the average of continuous variable between ASD and TD. Obtained p-value of metabolites and ratios were adjusted by the Benjamini-Hochberg (BH) procedure. PLS-DA was exploited to calculate VIP values of metabolites or ratios via using SIMCA (v14.1). PLS-DA plots were used to draw metabolites profiling of the two groups. The profiling differences between the two groups were tested by PERMANOVA, with $p < 0.05$ as significant. Differential metabolites or ratios between the two groups were determined by employing a threshold of $p < 0.05$, FDR <0.1 and VIP >1. ROC analysis was exploited to test the performance of potential markers for ASD.

Microbial profiling

Relative abundances of the GM genera were analyzed using α-diversity and β-diversity analyses with QIIME (v2.0). The values of α-diversity were presented as the Chao index and Shannon index. The values of β-diversity were measured using PCoA. PCoA plots were

used to draw microbial profiling of the two groups. The profiling differences between the two groups were tested by PERMANOVA, with $p < 0.05$ as significant. Comparison of Chao index, Shannon index and microbial relative abundance between the two groups were conducted via Wilcoxon rank-sum test, with $p < 0.05$ as significant. Differential genera were determined by the MaAsLin2 and LEfSe algorithms followed by BH procedure, with $p < 0.05$, FDR <0.1 as significant. For MaAsLin2, the ''LM (linear model)'' method and ''CLR (centered log ratio)'' normalization were used.[32]

Genetic profiling
Gene abundance was presented as count, and pathway abundance was calculated by summing relative gene abundances. Differential genes or pathways between the two groups were determined by Wilcoxon rank-sum test followed by BH procedure, with $p < 0.05$, FDR <0.1 as significant.

Integrated analysis
Pearson analysis was utilized to test association between metabolites, ratios, genera, genes or pathways, with $p < 0.05$ as significant. Before Pearson analysis, INT was performed to achieve normally distributed data after adjusting for confounders.

ADDITIONAL RESOURCES

No other additional resources.